

University of Groningen

Polymer and nanoparticles flooding as a new method for Enhanced Oil Recovery

Druetta, P.; Picchioni, F.

Published in:
Journal of Petroleum Science and Engineering

DOI:
[10.1016/j.petrol.2019.02.070](https://doi.org/10.1016/j.petrol.2019.02.070)

IMPORTANT NOTE: You are advised to consult the publisher's version (publisher's PDF) if you wish to cite from it. Please check the document version below.

Document Version
Publisher's PDF, also known as Version of record

Publication date:
2019

[Link to publication in University of Groningen/UMCG research database](#)

Citation for published version (APA):
Druetta, P., & Picchioni, F. (2019). Polymer and nanoparticles flooding as a new method for Enhanced Oil Recovery. *Journal of Petroleum Science and Engineering*, 177, 479-495.
<https://doi.org/10.1016/j.petrol.2019.02.070>

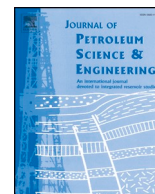
Copyright

Other than for strictly personal use, it is not permitted to download or to forward/distribute the text or part of it without the consent of the author(s) and/or copyright holder(s), unless the work is under an open content license (like Creative Commons).

Take-down policy

If you believe that this document breaches copyright please contact us providing details, and we will remove access to the work immediately and investigate your claim.

Downloaded from the University of Groningen/UMCG research database (Pure): <http://www.rug.nl/research/portal>. For technical reasons the number of authors shown on this cover page is limited to 10 maximum.



Polymer and nanoparticles flooding as a new method for Enhanced Oil Recovery

P. Druetta*, F. Picchioni

Department of Chemical Engineering, ENTEG, University of Groningen, Nijenborgh 4, 9747AG, Groningen, the Netherlands



ARTICLE INFO

Keywords:

EOR
Polymer
Nanotechnology
Reservoir simulation

ABSTRACT

A new Enhanced Oil Recovery (EOR) method is proposed by combining the effects of a traditional polymer flooding and exploiting the advantages that nanotechnology presents in the oil industry. Thus, a novel technique is introduced and applied to a 2D reservoir model with a two-phase, five-component system (aqueous, oil phases and water, hydrocarbon, polymer, nanoparticles and salt). For the polymer characterization, a novel approach is presented considering the polymer's architecture and its degradation in order to calculate the physical properties, which has never been reported in reservoir simulation. The presence of the nanoparticles affects mainly the rheological behavior and the wettability of the rock, increasing the oil phase mobility. Moreover, negative effects such as particle aggregation and sedimentation are also modeled using a novel formulation in reservoir simulation. The combined action of polymers and nanoparticles allowed increasing the recovery factors beyond standard EOR processes, and it represents a suitable alternative to replace traditional combined methods, such as Surfactant-Polymer (SP) or Alkaline-Surfactant-Polymer (ASP). This is due to the fact that the nanoparticles act, to a greater or lesser extent, on the wettability, rheological and interfacial properties of fluids and rock formation, which is complemented with the polymer's viscosifying properties. Moreover, economical factors could also render this technique more attractive, since the nanoparticles' associated costs are substantially lower than those from surfactant flooding. This simulation proves the potential of nanotechnology as a mean to boost traditional EOR techniques in order to further increase the operative life of mature oil fields.

1. Introduction

The main objective in Enhanced Oil Recovery processes is to alter the fluid and/or rock properties in order to diminish the oil saturation below the residual (S_{or}) after waterflooding (Dake, 1978; Morrow, 1987; Satter et al., 2008). Even though nanotechnology is not an EOR technique *per se*, the unique features found at the nanoscale allow boosting and improving the performance of current methods, modifying parameters which in the end result in an increase in the oil recovered. Therefore, the main objective of the nanotechnology assisted EOR processes is acting on one (or several) of the following factors: mobility control using viscosity-increasing water/polymer/nanoparticles solutions; altering the rock wettability; interfacial tension (IFT) reduction by adding surfactants; and lowering the oil viscosity by means of nanocatalysts which react at high temperatures, producing lighter fractions easier to recover.

The use of standards technologies in EOR allowed increasing the performance of oil fields after waterflooding. Although the recovery

factor was increased, decreasing the residual oil saturations, a significant percentage of the original oil in place (OOIP) remains still trapped even after the profitable limit of standard EOR processes. The attention was focused then on boosting the efficiency of these methods. During the last 15 years researchers have looked for ways to increase the efficiency of these methods, and the response came through from the nanotechnology, thanks to the exceptional properties of the materials at these length scales. By injecting nanoparticles in both waterflooding and polymer flooding processes, it has been possible to increase the recovery efficiency. Therefore, the development of a polymer flooding model enhanced by means of nanotechnology is discussed during this paper. The oil recovery process in the 2D oil field is thoroughly discussed to simulate a two-phase, five-component flow.

1.1. Nanotechnology in EOR

Several authors have studied the transport of nanoparticles in porous media and their application to EOR processes (Maurya and

* Corresponding author.

E-mail address: p.d.druetta@rug.nl (P. Druetta).

URL: <http://www.rug.nl/research/product-technology/> (F. Picchioni).

Nomenclature		ϕ	Formation Porosity
Ad	Component Adsorption [1/day]	Ω	Reservoir Domain
c_r	Rock Compressibility [1/Pa]	<i>Superscripts</i>	
\mathcal{D}	Dispersion Tensor	a	Aqueous Phase
f	Number of arms (polymer)	c	Capillary
K	Absolute Permeability [mD]	H	Water-Oil System (no Chemical)
k_r	Relative Permeability	j	Phase
p	Reservoir Pressure [Pa]	$\langle n \rangle$	Time-Step
p_{wf}	Bottomhole Pressure [Pa]	o	oil Phase
q	Flowrate [m^3/day]	r	Residual
r_w	Well Radius [m]	<i>Subscripts</i>	
S	Phase Saturation	i	Component
s	Well Skin Factor	in	Injection
u	Darcy Velocity [m/day]	m, n	Spatial Grid Blocks
v	Nanoparticles Adsorption	np	Nanoparticle Component
V	Volumetric Concentration	p	hydrocarbon Component
z	Overall Concentration	pol	Polymer Component
<i>Greek Letters</i>		s	Salt Component
Γ	Domain Boundary	t	Total
λ	Phase Mobility	w	Water Component
μ	Absolute Viscosity [Pa·s]		
σ	Interfacial Tension [mN/m]		

Mandal, 2016; Onyekonwu and Ogolo, 2010). However, to the extent of our knowledge, there are no reports in the literature on the numerical simulation of a combined process of chemical EOR with nanoparticles, so it is deemed that it is of vital importance to understand how these methods work. As in the previous case with the SP flooding, the combination of two agents for EOR cannot be considered only as the sum of independent elements, but the interaction between them must also be considered. In the case of nanoparticles in polymer solutions this cannot be avoided (Maurya and Mandal, 2016; Berret et al., 2004; Choi et al., 2017). An example of this interaction is the diffusion of the nanoparticles into the porous medium. The Stokes-Einstein equation describes this phenomenon for nanoparticles in pure fluids, at low concentrations. However, the presence of the polymer molecules and their interactions with the particles affects this process, coupled with the fact that, at higher concentrations, the interaction among the nanoparticles cannot be avoided.

The study of nanoparticles in porous media was also analyzed in a novel way for the cases of CO₂ storage and EOR by CO₂ by Sbai (Sbai and Azaroual, 2011). A 2D simulator was developed for both homogeneous and heterogeneous media, taking into account the particulate release, migration, and capture in two-phase flow systems. This simulator was validated by laboratory tests and proved useful for testing the efficiency of nanoparticles in both two-phase CO₂ storage (i.e., CO₂ and water) and EOR (CO₂ and oil) processes. Sbai took into account more physical phenomena than the previous models, as well as the presence of salt as an extra component, although the influence of nanoparticles on the carrier phase properties was not considered, which affects the efficiency of the EOR process and mobility ratio. Nevertheless, this model proved to be useful in designing fluids' re-injection and production schemes as well as to study particulate transport processes in CO₂ injection projects.

This simulator is based on a previous model, in which surfactant has been replaced by nanoparticles. To the best of our understanding, there is no commercial simulator in the literature including a specific module of nanoparticles for EOR recovery processes. In addition, these simulators do not include a polymer degradation module which allows to calculate the physical properties of the aqueous phase as the polymer chain-scission takes place and its molecules lose their viscosifying

efficiency. Considering the academic simulators described before, they are based mainly on 1D models, which do not take account of areal recovery efficiency, a key parameter in field operations. In addition, these simulators were intended to primarily study the transport of nanoparticles in porous media, without focusing on EOR recovery processes. The two-dimensional simulators presented study EOR or CO₂ storage methods, performing a detailed study of the retention of the nanoparticles, without studying how they affected the phases properties (i.e., rheology). Moreover, they do not include a formulation that allows to modify the size of the particles as a function of time due to aggregation phenomena (Anne-Archard et al., 2013; Berret et al., 2004; Brunelli et al., 2013), nor they include the presence of another sweeping agent for EOR (i.e., polymer). Finally, the expansion of the model to three-dimensional fields may cause the system to lose numerical efficiency since larger non-linear systems of equations must be solved. This is the reason why this study is based on a two-dimensional system and therefore it is recommended that a further expansion to a three-dimensional field must be carried out, especially for the cases when the vertical permeability cannot be neglected with respect to horizontal ones. Hence, the computational cost is increased but the results may not show a significant difference in comparison to two-dimensional fields. The object of this study is the optimization in the employment of existing agents or in the efficiency of new techniques for EOR. Once the validity of these last ones is proved, the adaptation to 3D models is straightforward.

1.2. Environmental effect of nanoparticles

Nanotechnology has showed during the last years to have a promising future in improving the economics in several disciplines, such as transportation, agriculture, energy and health. The potential benefits of nanotechnologies have been welcomed as far as health and environmental aspects are concerned (for instance in water sanitation). However, some concerns have been noted since the features that are being exploited (such as high surface reactivity and ability to cross cell membranes) might also have a negative impact on human health and the surrounding environment, resulting in greater toxicity. Concerns about possible long-term side effects associated with medical

applications and the biodegradability of nanomaterials have been expressed (Druetta et al., 2018).

During the last 15 years, many nanomaterials have moved into the marketplace with direct and indirect effects in the society. Nonetheless, up to this moment there are only minimal data on the nanomaterials exposure effect on the human health and environment in a long-term scale. Moreover, the results of some studies showed some concerns about the effect of these nanomaterials. In addition, there exists little information about the manufacturing, usage and disposal of the nanomaterials and any associated risks from the exposure to them. Moreover, there are not still proper detection methods, measurement, analyzing and tracing tools for nanomaterials. Regarding EOR processes, there has been studies about nanoparticles being used as adsorbent/catalysts for heavy oil recovery, which is a new and challenging chemical process. However, there exist many challenges that should be analyzed to understand and cover all the aspects of the nanoparticles application. In these, it was reported that a percentage of injected nanoparticles into the formation are deposited inside the porous media, and will remain in-situ for many years, and so far no study was performed on the long term environmental effect of these nanocatalysts. On the other side, some portion of the injected nanoparticles is recovered with the upgraded oil. Thus, every aspect of the utilization of the nanomaterial should be fully evaluated beforehand by experimental and modeling analysis. Additionally, in the operational side, the possibility of groundwater contamination by the nanocatalysts should be considered as a potential operational failure risk. Desirable sustainable nanocatalysts should present higher activity, higher selectivity, efficient recovery as well as durability and recyclability in a cost-effective process so as to decrease the impact on the environment. Currently, there are groups working on developing and implementing sustainable nanoparticles, which could have much less environmental impact compared to the synthesized or commercially available nanoparticles (Druetta et al., 2018).

1.3. Aim of this work

The paper presents a new simulator for nanotechnology-boosted chemical EOR processes, specifically combining these with a polymer flooding. This renders a two-phase, five-component model which represents the first numerical simulator of nanotechnology enhanced chemical EOR process with polymers. Regarding the nanoparticles, the simulator takes into account all the possible effects, such as aggregation, retention, rheology, and changes in permeability and porosity. With respect to the polymer, it includes a novel relationship between architecture and phase properties, focusing on the viscoelasticity and rheology (Graessley et al., 1976; Berry, 1968, 1971; Graessley, 1977). Furthermore, the influence between both components has been included, which mainly affect the rheology and the diffusion coefficient of the nanoparticles. Moreover, the aqueous phase viscosity formulation takes into account the influence of all the components present in the phase, which to the extend of our knowledge, is not considered in previous commercial and academic simulators. This has led to a new simulator which is able to assess the benefits of nanotechnology with chemical EOR processes. The highly non-linear system of equations is solved using a second order discretization scheme with a flux limiter function in the mass transport equations so as to minimize numerical diffusion and dispersion phenomena.

1.4. Physical model

The physical model is composed by a 2D domain (Ω), representing an oil field with determined physical properties, i.e., an absolute permeability tensor (K), the rock compressibility (c_r), and the porosity field (ϕ). The flow is considered isothermal and incompressible. Darcy's law is valid and gravitational forces are negligible (Bidner and Savioli, 2002; Lake, 1989; Sheng, 2011). The combined nanoparticles-polymer EOR flooding involves the flow of fluids in a two-phase (aqueous and oil), multicomponent (water, salt, polymer, nanoparticles and

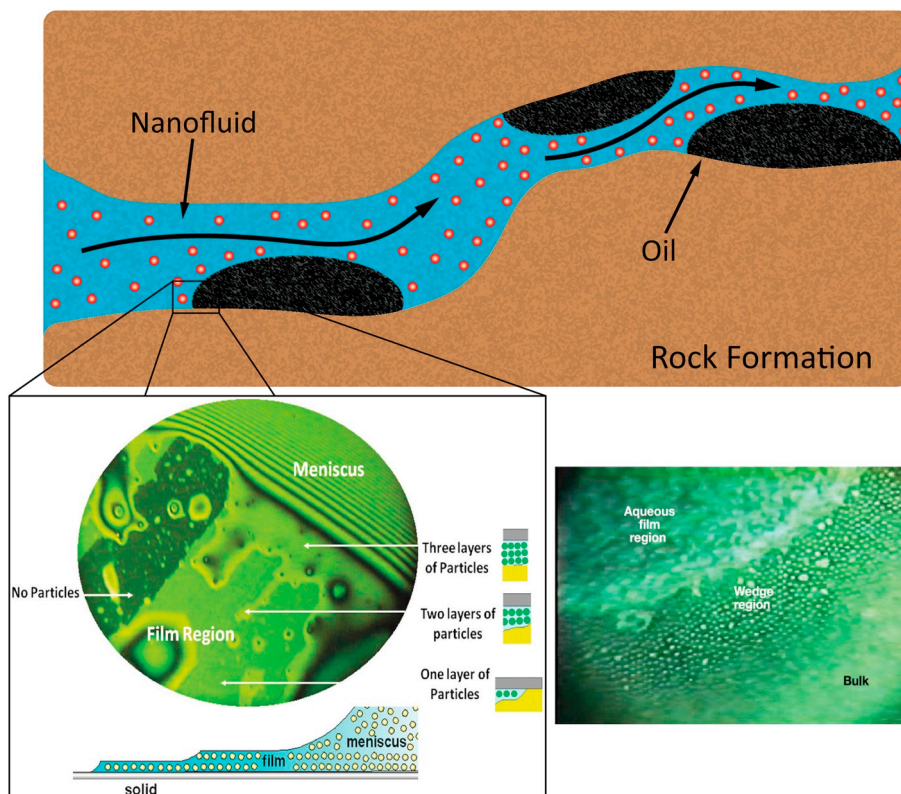


Fig. 1. Scheme of a nanoparticles flooding and wedge formation in oil drops (Adapted from: Wasan and Nikolov (Wasan and Nikolov, 2003; Nikolov et al., 2010)).

hydrocarbon) system. These components may be mixtures of a number of pure ones, since hydrocarbon is essentially a mixture of many hydrocarbons, and the water may contain dissolved minerals (other than the salt itself), and the polymer is composed by a number of molecules of different lengths and architectures (Sheng, 2011). The properties of the polymer are determined by its average molecular weight, assuming that all the molecules are identical, which means the polydispersity index (PDI) equal to unity. Moreover, in this simulator also the structure of the polymer plays an important role: linear or branched architectures affect the rheology of the aqueous phase. This is determined by the molecular weights of backbone and arms, and the number of the latter. The nanoparticles also affect the water phase and the rheology and this is a function of the concentration and the size of the nanoparticles. With respect to the latter, aggregation mechanisms tend to increment the average size of the particles, modifying its rheological influence on the water phase. The way nanoparticles affect the recovery process is based on the work developed by Wasan and Nikolov (Fig. 1). (Wasan and Nikolov, 2003; Kondiparty et al., 2011; Wasan et al., 2011; Nikolov et al., 2010)

The mathematical description of the system is represented by a number of strongly non-linear partial differential equations complemented by a set of algebraic relationships describing the physical properties of fluids and rock, which are: aggregation of nanoparticles, degradation of polymer molecules, interfacial tension, residual phase saturations, relative permeabilities, rock wettability, phase viscosities, capillary pressure, adsorption and retention of both polymer and nanoparticles onto the formation, inaccessible pore volume (IAPV), disproportionate permeability reduction (DPR), nanoparticles-polymer interactions, and dispersion.

1.5. Mathematical model

The characteristics of chemical EOR methods, including nanotechnology transport in porous media, render a system in which the phases' properties depend on the concentration of the components, which results in a strongly non-linear system and thus traditional reservoir approaches (e.g., black-oil) are not suitable. The compositional flow, on the other hand, allows the simulation of a multiphase, multi-component system in which the properties can be expressed as a functions of the concentrations. This numerical model is based on a previous one developed also to simulate chemical EOR flooding (Druetta et al., 2017; Druetta and Picchioni, 2018), which was validated against an academic simulator (UTCHEM) in a series of 2D flooding processes (Chen et al., 2006; Barrett et al., 1994; Kamalyar et al., 2014). Therefore, the Darcy, mass conservation and aqueous pressure equations yield,

$$\vec{u}^j = -\frac{K}{\mu^j} \cdot \vec{\nabla} p^j; j = o, a \tag{1}$$

$$\frac{\partial(\phi z_i)}{\partial t} + \nabla \cdot \sum_j V_i^j \cdot \vec{u}^j - \nabla \cdot \sum_j \underline{D}_i^j \cdot \nabla \cdot V_i^j = -\frac{\partial(\phi A d_i)}{\partial t} + q_i; \tag{2}$$

$i = p, np, w, s, pol$

$$\phi_c \frac{\partial p^a}{\partial t} + \vec{\nabla} \cdot (\lambda \cdot \nabla p^a) = \frac{\partial}{\partial t} \left(\phi \cdot \sum_i A d_i \right) - \vec{\nabla} \cdot (\lambda^o \cdot \nabla p_c) + q_t \tag{3}$$

2. Physical properties

The goal of this section is to present only the physical properties modified by the presence of polymer and nanoparticles, focusing on the rheological properties being modified by both agents as well as the modification of the nanoparticles' diffusion coefficient by the presence of the polymer. Thus, the following phenomena are also considered using models described in the literature: residual saturations, relative

permeabilities, interfacial tension, disproportionate permeability reduction (DPR), inaccessible pore volume (IAPV) and capillary pressure (Druetta et al., 2017; Delshad et al., 2000).

2.1. Chemical component partition

Regarding the nanoparticles' phase behavior, it is assumed a similar concept to the partition coefficient used for surfactants. Depending on their wettability, HLPN (hydrophobic and lipophilic polysilicon nanoparticles), NWPN (neutral wet polysilicon nanoparticles) or LHPN (lipophobic and hydrophilic polysilicon nanoparticles), the nanoparticles will tend to be present in the oil, mixed or aqueous phase, respectively. The phase partition analysis adopted is similar to the model employed for surfactant, thus,

$$\text{Solubilization Coefficient} = L_{pnp}^a = \frac{V_p^a}{V_{np}^a} \tag{4}$$

$$\text{Swelling Coefficient} = L_{wnp}^o = \frac{V_w^o}{V_{np}^o} \tag{5}$$

$$\text{Partition Coefficient} = k_{np} = \frac{V_{np}^o}{V_{np}^a} \tag{6}$$

For the purpose of this paper, it is considered that both hydrocarbon and water remain in their respective phases ($(L_{pnp}^a = L_{wnp}^o = 0)$). Moreover, in the combined flooding it will be used only LHPN particles ($k_{np} \approx 0$). The other two phase behavior auxiliary relationships come from the salt and polymer, which are assumed to be present only in the aqueous phase ($V_s^o = V_{pol}^o = 0$).

2.2. Aggregation of nanoparticles

There is extensive literature research and experiments showing that nanoparticles in solutions may aggregate until they reach a critical size and begin to sediment (Anne-Archard et al., 2013; Berret et al., 2004; Brunelli et al., 2013; Pranami, 2009; Capco and Chen, 2014). The aggregation of nanoparticles is the formation of clusters by particles, or when small clusters aggregate to form a bigger ones due to the balance of forces in the system explained, for example, by the Derjaguin-Landau-Verwey-Overbeek (DLVO) theory (Fig. 2). The gradual increase in the size of these clusters can cause the sedimentation of the nanoparticles in the porous medium, separating them from the nanofluid, which it is an undesired effect. On the other hand, clusters can also be broken and generate smaller ones if the diameter or number of

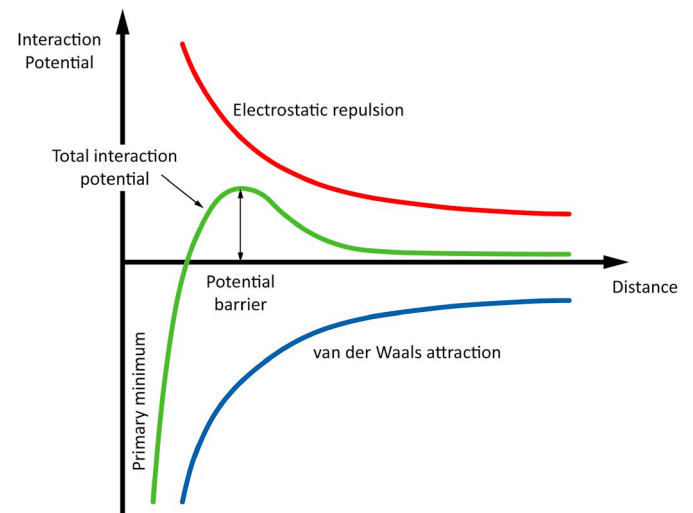


Fig. 2. Forces at the molecular scale affecting the nanoparticles.

nanoparticles in the same reaches a critical limit (Fig. 3). (Jiang et al., 2010; Kang et al., 2012; Li, 2016; Markus et al., 2015; Markutsya, 2008; Kohli, 2013)

This phenomenon is considered in the simulation with nanoparticles. It has been adopted, as in the case of the degradation of polymer molecules, an exponential law to take into account the change in the average diameter of the nanoparticles as a function of time and their injection in the reservoir. This size is updated during the flooding process so as to recalculate all the related parameters (see point 2.5). In addition, based on the work of Jiang (Jiang et al., 2010), it is considered a maximum possible size of the cluster of nanoparticles, above which it undergoes a splitting process in identical clusters of smaller size, with the properties being calculated for this new average diameter.

$$\frac{dDia_{np}}{dt} = K_{aggreg} \cdot Dia_{np} \quad (7)$$

2.3. Phase viscosities

The polymer is added to the aqueous phase to increase its viscosity and thus improve the mobility ratio, avoiding the phenomenon of water fingering (Sheng, 2011; Dake, 1978; Lake, 1989). Nanoparticles are also used to increase the viscosity of nanofluids and several correlations were presented over the years to calculate their viscosity. Since Einstein's original work, which was used for low concentrations, studies have been expanded to take into account other factors, among others: the size and type of the nanoparticles, temperature and the characteristics of the carrier fluid (Duan et al., 2011; Khandavalli and Rothstein, 2014; Meyer et al., 2016; Mishra et al., 2014; Saito et al., 2012; Jia-Fei et al., 2009; Maghzi et al., 2013). A step-wise procedure was adopted in the new simulator to calculate the viscosity of the aqueous phase. The first step consists in calculating the phase viscosity considering only the TDS. During this paper a modification to the classical approach was introduced (e.g., UTCHEM (Delshad et al., 2000)), considering the dependence on the salt in the pure water/brine viscosity (Pal, 1020; Rudyak, 2013; Shakouri et al., 2017). The first step is to determine the viscosity ratio between a linear polymer used as reference, and a branched one with the same total molecular weight. There are several correlations allowing determining this relationship based on the number and molecular weight of the arms and backbone (Graessley et al., 1976; Berry, 1967, 1971; Graessley, 1977; Phillies, 1987; Shanbhag, 2012). Equation (8) is used in the simulator to calculate this ratio,

$$g_{viscosity} = \frac{1}{(1 + \rho \cdot f)^3} [1 + 2f \cdot \rho + (2f + f^2)\rho^2 + (3f^2 - 2f)\rho^3] \quad (8)$$

where f is the number of arms of the polymer and ρ is the relationship between the molecular weights of the arms and backbone. (Teraoka, 2002) This relationship is calculated in each time-step since the simulator has the possibility to choose different degradation rates for arms and backbone, rendering this relationship as a time dependent function. The number of arms depends on the polymer used for the EOR process and in this study the polymers developed by Wever (Wever et al., 2013) were used as example, who synthesized branched polymers up to a maximum of 17 arms. Next, the viscosity of the aqueous phase at zero shear-rate is calculated using a formulation based on the total molecular weight.

$$\mu_{0sr} = \mu_w \left\{ 1 + [k_1(g_v, f) \cdot [\eta] \cdot V_{pol}^a + k_2(g_v, f) \cdot [\eta] \cdot V_{pol}^{a^2} + k_3(g_v, f) \cdot [\eta] \cdot V_{pol}^{a^3}] C_{SEP}^{Sp} \right\} \quad (9)$$

Finally, the influence of nanoparticles is considered in both phases, which depends primarily on the type of particles used. There are several proposed correlations to calculate the nanofluid relative viscosity. In this simulator, since aggregation and retention phenomena are involved, a formulation was used considering both the concentration and

nanoparticles' size in the phase (Delshad et al., 2000; Litchfield and Baird, 2006; Maurya and Mandal, 2016; Mikkola, 2012).

$$\mu_{np} = \mu_{cf} \cdot [1 + (2.5 + \eta_1 e^{-Dia_{np}/d_w}) \cdot V_{np}^a + (6.2 + \eta_2 e^{-Dia_{np}/d_w}) \cdot V_{np}^{a^2}] \quad (10)$$

where V_{np}^a is the concentration of particles in the phase, Dia_{np} is the average size of the nanoparticles or clusters, d_w is the diameter of the carrier fluid molecules and $\eta_{1,2}$ are correlation constants. It is noteworthy that the present simulator does not incorporate the effects that can be found with associating polymers and nanoparticles. (Zhu et al., 2014; Choi et al., 2017; Saito et al., 2012) It is deemed that further research on the topic should be carried out so as to be able to elaborate mathematical models considering this interaction to calculate the viscosity of semi-dilute polymer solutions with nanoparticles.

2.4. Diffusion of nanoparticles

The diffusion of the nanoparticles can significantly affect their transport and how they alter the properties of the phases, which ultimately changes the efficiency of the EOR process. In previous reported numerical models, the influence of other molecules in the diffusion process of the particles has not been taken into account and, in addition, the influence of the concentration of the particles in the mentioned process was not taken into account (Sbai and Azaroual, 2011). In this simulator it is considered this phenomenon when the particles are in the aqueous phase, using the correlation developed by Phillies (1987), whilst the diffusion factor of those present in the oil phase will only be corrected based on their concentration. The starting point for the study of this phenomenon is Brownian diffusion coefficient by the Stokes-Einstein equation. The latter is valid for low concentrations, so the first correction consists in adjusting the coefficient for higher concentrations.

$$D_{np}^a = \frac{k_B T}{3\mu_{cf} \pi Dia_{np} f_{corr}} \quad (11)$$

$$f_{corr} = (1 - V_{np}^a)^{-6.55} \quad (12)$$

This coefficient is then modified based on a correlation which takes into account both the presence of the polymer and its properties (i.e., architecture, chemical formula, radius of gyration and molecular weight). The radius of gyration of a molecule depends on its structure as well as its chemical composition and molecular weight. Therefore, the first step is to establish a methodology to calculate the polymer's radius of gyration as a function of time in the flooding process (Omari et al., 2009).

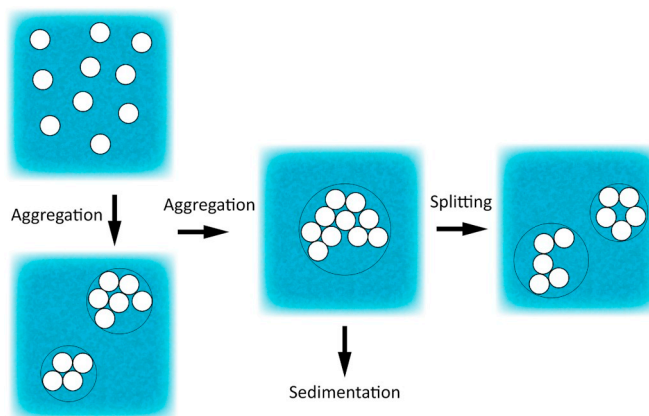


Fig. 3. Scheme of the aggregation mechanisms of nanoparticles and their subsequent splitting.

$$R_{g,linear} = b_{rg} \cdot \left(\frac{M_{w,bb} + f \cdot M_{w,arm}}{M_{w,mon}} \right)^{0.588} \quad (13)$$

where b_{rg} is the bond or segment length and $M_{w,mon}$ is the molecular weight of the monomer. Similarly to what was done in the phase viscosities' calculation (see Eq. (8)), the radius of gyration of the branched polymer must be calculated based on the architecture of the molecules. For this purpose, a relation similar to the previous one was adopted, which is only function of the polymer's number of arms (Fig. 4).

$$g_{rg} = \frac{3f - 2}{f^2} \quad (14)$$

Finally, the diffusion coefficient of the nanoparticles is calculated using a step-wise function based on the size of the nanoparticles, their radius of gyration and the overlapping concentration, based on the analysis described by Flory (Kohli, 2013; Teraoka, 2002; Dong et al., 2015; Kohli and Mukhopadhyay, 2012; xian Li et al., 2016; Metin, 2012).

$$\phi^* = \frac{3(M_{w,bb} + f \cdot M_{w,arm})}{4\pi\rho_{pol}N_{Av}R_g^3} \quad (15)$$

$$\chi = R_{g,pol} \left(\frac{V_{pol}^a}{\phi^*} \right)^{-0.76} \quad (16)$$

$$D_{NP}^a \Rightarrow \left\{ \begin{array}{ll} D_{NP}^a \cdot e^{-\alpha_D \left(\frac{Dia_{NP}}{2\chi} \right)^{\delta_D}} & \text{if } \left(\frac{Dia_{NP}}{2} \right) \leq R_g \\ D_{NP}^a \cdot e^{-\alpha_D \left(\frac{R_g}{\chi} \right)^{\delta_D}} & \text{if } \left(\frac{Dia_{NP}}{2} \right) \geq R_g \end{array} \right. \quad (17)$$

where ρ_{pol} is the density of the polymer, N_{Av} is the Avogadro number, and α_D and δ_D are constants. The diffusion coefficient is then a function of time since it depends on the molecular weight of the polymer, which varies due to the degradation mechanisms.

2.5. Retention and adsorption

The adsorption process occurs when particles or polymer molecules form onto the surface of the formation rock. This irreversible phenomenon will cause a loss of the chemicals in the phases in the porous media, making the whole process economically unfeasible in case of high rates of adsorption. This is due to the fact that extra EOR agents would be necessary and the interfacial properties will be decreased. (Delshad et al., 2000).

Similarly to what happens in a combined EOR flooding (Sheng, 2011), a process of competitive adsorption is considered since the polymer molecules cover part of the rock formation's surface, thus there will be a smaller area for the adsorption of nanoparticles to take place. The numerical formulation involves two factors, one affecting the polymer's adsorption in case the nanoparticles are injected first, and the second factor for the latter, if the polymer is injected in the first place. In this paper only the phenomena of retention and adsorption of nanoparticles is presented. Particle capture and release will also alter the rock formation properties (i.e., porosity and permeability) provided the size of the nanoparticle is larger or of the same order that the pore size or if a large volume of particles accumulate (Metin, 2012; Ju and Fan, 2009, 2013; Taborda et al., 2017; Zhang et al., 2015). The net rate loss of nanoparticles in the porous medium is quantified in Eq. (3) and it can be expressed as follows (Sbai and Azaroual, 2011; Ju and Fan, 2009),

$$Ad_{np} = (F_{SP} \cdot v_1 + v_2 + v_3) \quad (18)$$

where v_1 represents the volume of the nanoparticles in contact with the phase j available on the pore surfaces per unit bulk of the porous medium, v_2 is the volume of the nanoparticles entrapped in the pores of the phase j per unit bulk of porous medium due to plugging and

bridging, and v_3 is the release rate of nanoparticles from pore walls by colloidal forces, considering both the salinity of the system and the possible charge of the nanoparticles. The last term represents an extension of the models previously reported and it is based on the work developed by Sbai. (Sbai and Azaroual, 2011) The first term can be expressed by a critical velocity for surface deposition. Below this value only the phenomenon of retention of the particles in the porous formation occurs, and above it a combination of effects of retention and entrainment takes place. The model for expressing v_1 is according to a step-wise function (or Heaviside) based on the critical velocity.

$$v_1^{(n)} \Rightarrow \left\{ \begin{array}{ll} \alpha_1 \cdot u^j \cdot V_{np}^a & \text{if } u^j \leq u_{crit}^a \\ \alpha_1 \cdot u^j \cdot V_{np}^a - \alpha_2 \cdot v_1^{(n-1)} \cdot (u^j - u_{crit}^j) & \text{if } u^j \geq u_{crit}^a \\ v_1^{(n)} > 0 \quad \forall \Omega & \end{array} \right. \quad (19)$$

where α_1 is the coefficient for surface retention of the nanoparticles in the phase j in the rock formation, α_2 is the coefficient for entrainment of the nanoparticles in the phase j and v_{crit} is the critical velocity for the phase j . The data necessary to calculate the critical velocity as a function of the nanoparticle size were obtained from Ju (Ju and Fan, 2009, 2013; Ju et al., 2006) (Fig. 5). This study considers spherical-shaped particles and clusters but it is deemed that, in future models, the critical velocity should be also expressed as a function of the shape as well. It is worth mentioning on this term that retained particles on the rock formation surface may desorb due to hydrodynamic forces and then be subsequently adsorbed on different sites or entrapped at pore throats, further in the reservoir.

$$u_{crit}^j [m/day] = 0.00992736 \cdot Dia_{NP} [nm] + 0.0009936 \quad (20)$$

For the term v_2 is used a formulation similar to the term of retention in v_1 , and is expressed according to the following function,

$$v_2^{(n)} \Rightarrow \left\{ \begin{array}{ll} \alpha_3 \cdot u^j \cdot V_{np}^a & \\ v_2^{(n)} > 0 \quad \forall \Omega & \end{array} \right. \quad (21)$$

where α_3 is the pore blocking constant in the phase j . Finally, the term v_3 is calculated according to Sbai (Sbai and Azaroual, 2011) and it is a function of the salinity (TDS) in the medium.

$$v_3^{(n)} \Rightarrow \left\{ \begin{array}{ll} -\alpha_4 \cdot v_1^{(n)} \cdot (C_{sc} - V_s^a) & \\ v_3^{(n)} > 0 \quad \forall \Omega & \end{array} \right. \quad (22)$$

where α_4 is the constant rate of colloiddally induced mobilization of in-situ nanoparticles. Equation (22) means that colloidal release of particles from phase j is limited by the critical salinity C_{sc} . This depends as

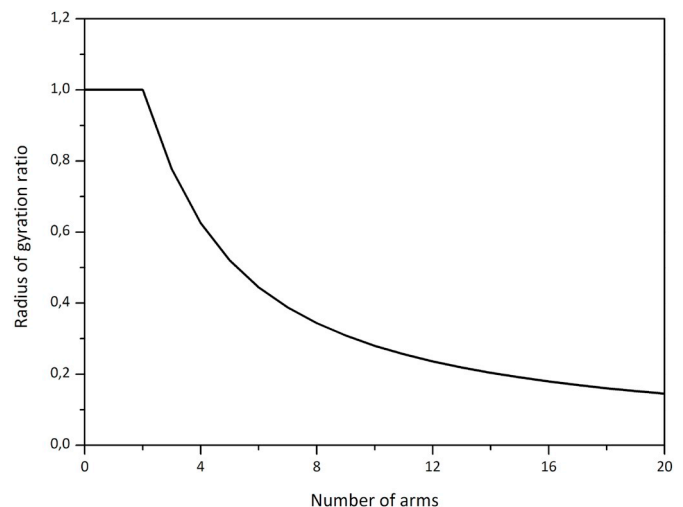


Fig. 4. Radius of gyration ratio g_{rg} as a function of the numbers of arms and the molecular weight relationship.

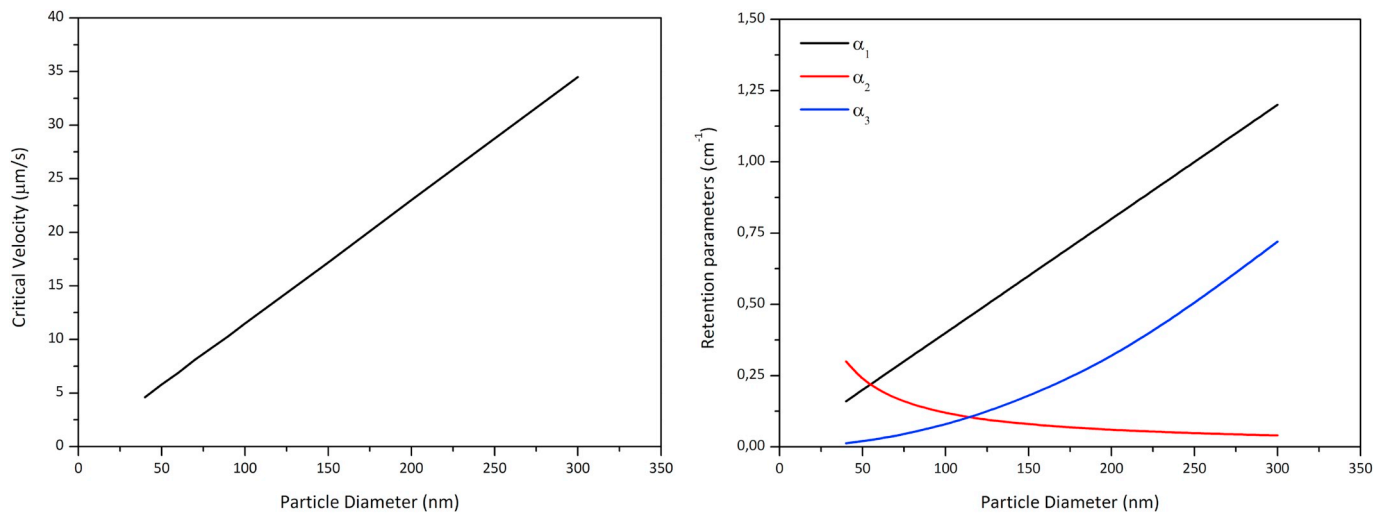


Fig. 5. Critical velocity (left) and retention parameters (right) as a function of the particle size.

Table 1
General parameters used for the simulations.

Geometrical Data of the Reservoir					
Length in axis X	500 m	Length in axis Y	500 m	Layer thickness	5 m
n_x	40/100 blocks	n_y	40/100 blocks		
Rock Properties					
Porosity	0.25	k_{xx}	200 mD	k_{yy}	200 mD
Initial Conditions					
S_o	0.70	S_o^r (EOR)	0.35	$S_a^{rH} = S_o^{rH}$	0.15
Simulation Data					
Total time	3,000 days	NP's inj. time	100 days	z_{npIN}	0.2
		Pol. inj. time	100 days	z_{polIN}	0.025
Physical Data of the Phases					
μ^{aH}	1 cP	μ^{oH}	10 cP	Oil density	850 kg/m ³
Water density	1,020 kg/m ³	IFT	50 mN/m		

Table 2
Physical data and operating conditions of the wells.

Physical Data					
Number of wells	2	Well radius	0.25 m	Skin factor	0
Operating Conditions					
Total flowrate	223 m ³ /day	Bottomhole pressure	55,160 kPa		

Table 3
Auxiliary parameters.

Interfacial Tension				Capillary Pressure				IAPV			
G_1	-1.7	G_2	-0.02	C	0	n	1	ϕ_{IAPV}	0.05		
Viscosity				Residual Saturation				Relative Permeabilities			
η_1	13.43	$\alpha_{1/2}$	0/0/1	T_1^o	-0.25	T_1^a	-0.50	k_r^{oH}	1	k_r^{aH}	0.2
η_2	38.33	dw	3×10^{-10} m	T_2^o	1.57	T_2^a	-0.70	e^{oH}	1.5	e^{aH}	1.5
DPR				Diffusion				EOR Agents			
$R_{k,cut}$	10	$b_{r,k}$	100	δ_D	0.89	ρ_{pol}	1300 kg/m ³	D_{np}	5 nm	K_{AGG}	5×10^{-4} 1/day
$c_{r,k}$	4.11			α_D	1.63	b_{rg}	0.16×10^{-9}	f_{arms}	16	$M_{w,pol}$	5×10^6 Da

well on the type of nanoparticles and the mineralogy of the rock formation.

One of the most important consequences of the mechanisms described herein is the modification of the properties of the porous medium. The nanoparticles sedimentation, adsorption and retention (by blocking and bridging) in the channels and throats affect the flowability and are one of main mechanisms of formation damage. (Druetta et al., 2018) The model developed by Ju (Ju and Fan, 2009, 2013; Ju et al., 2006) was chosen in this simulator to quantify this process. These mechanisms affect also the porosity of absolute permeability of the rock formation and they are independent of the variations by compressibility of the rock formation. The relative permeability modification is then calculated estimating the area of the porous medium covered by the nanoparticles. Thus, the modification can be calculated by a linear interpolation between two values: with no nanoparticles present, and when the entire surface in the medium is completely covered by the nanoparticles, adsorbed or entrapped in the rock formation and pore throats, reaching the maximum wettability change.

3. Results and discussion

3.1. Introduction

The goal of this simulator is to determine the advantages of using nanoparticles combined with a polymer EOR flooding, including a discussion of the possible injection strategies. The latter comprises also how the advantages of both polymer and nanoparticles can be employed in order to decrease the oil residual saturation, increasing the

Table 4
Results of the recovery process for different combined flooding schemes indicating the injection scheme.

Case	Oil recovered		Case	Oil recovered	
days	m ³	%OOIP	days	m ³	%OOIP
Pol. + NP (0–100/500–600)	66,340	35.4	NP + Pol. (0–400/300–400)	76,310	40.7
Pol. + NP (0–100/250–350)	67,730	36.1	Pol. + NP (0–100/100–200)	71,040	37.9
NP + Pol. (0–100/500–600)	60,590	32.3	Pol. + NP (0–100/50–150)	71,840	38.3
NP + Pol. (0–100/250–350)	69,980	37.3	NP + Pol. (0–400/150–250)	81,620	43.5
NP + Pol. (0–200/250–350)	73,410	39.2	NP + Pol. (0–400/50–150)	83,190	44.4

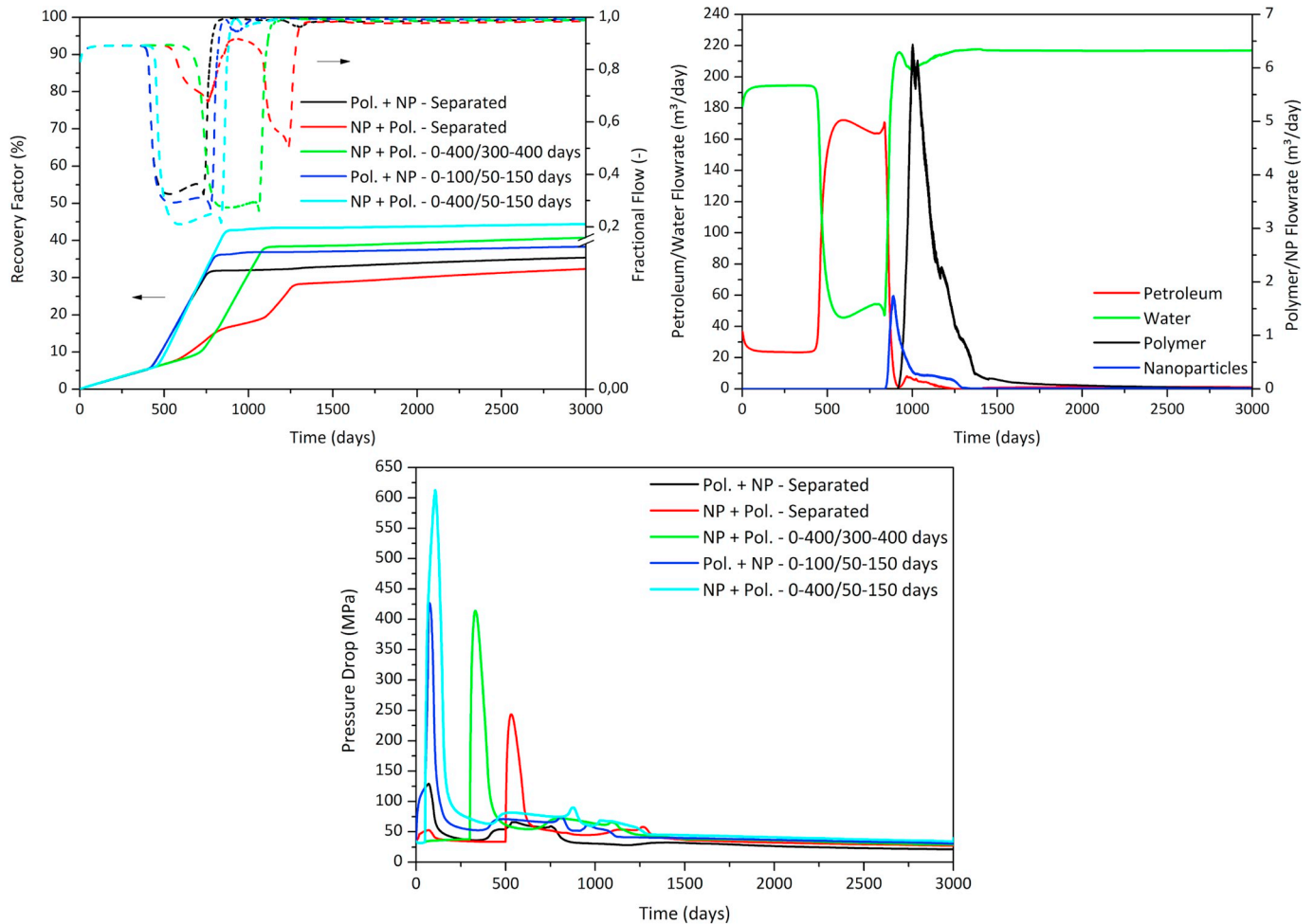


Fig. 6. Oil recovery, fractional flow (top left), flowrates for the optimum case (top right), and pressure drop (bottom) as a function of time for different combined EOR flooding schemes.

lifetime and production of existing mature fields. To the best of our knowledge, there are no combined flooding processes presented in the literature where the use of nanotechnology is introduced in order to enhance standard EOR processes.

3.1.1. Data

The simulation conditions and physical properties are established aimed at emulating an existing oil field apt for an EOR process with polymers and nanoparticles after a primary recovery (Tables 1–3). The rock is originally oil-wet, since one of the goals is to study the effect of LHPN particles in the rock's wettability. Furthermore, the grid has two possible configurations in order to study the simulator's behavior with large sparse block-triangular matrices (Druetta and Picchioni, 2019).

3.2. Polymer flooding enhanced by nanoparticles

The use of combined chemicals in a single EOR technique has been widely used and known for 20 years. Later on, these techniques were combined making use of the possible advantages and synergies of using chemicals together. The simulations, tests and field-scale applications evidenced that, when chemicals injected were separated by higher temporal gaps, the system tended to operate as two separate processes (Sheng, 2011). Polymers are mainly based on increasing the viscosity of the aqueous phase, decreasing the mobility ratio from a rheological point of view (Lake, 1989). Nanoparticles, on the other hand, though increase the viscosity of the carrying phase, enhance the recovery efficiency by decreasing the interfacial tension as well as by altering the wettability of the rock formation. Therefore, a combined use of nanoparticles with polymers can result in a new EOR technique with

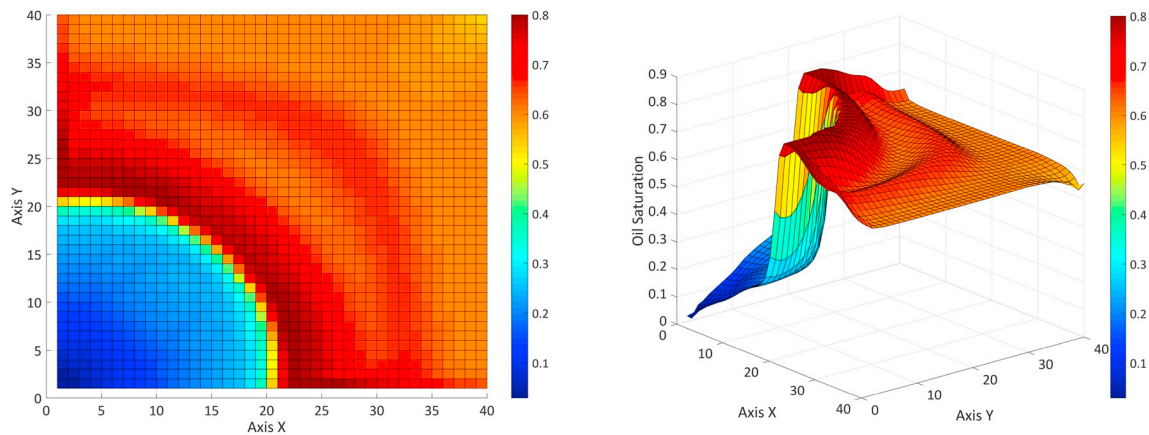


Fig. 7. Oil saturation after 500 days for the nanoparticles and polymer flooding (0–400/300-400 days) scheme.

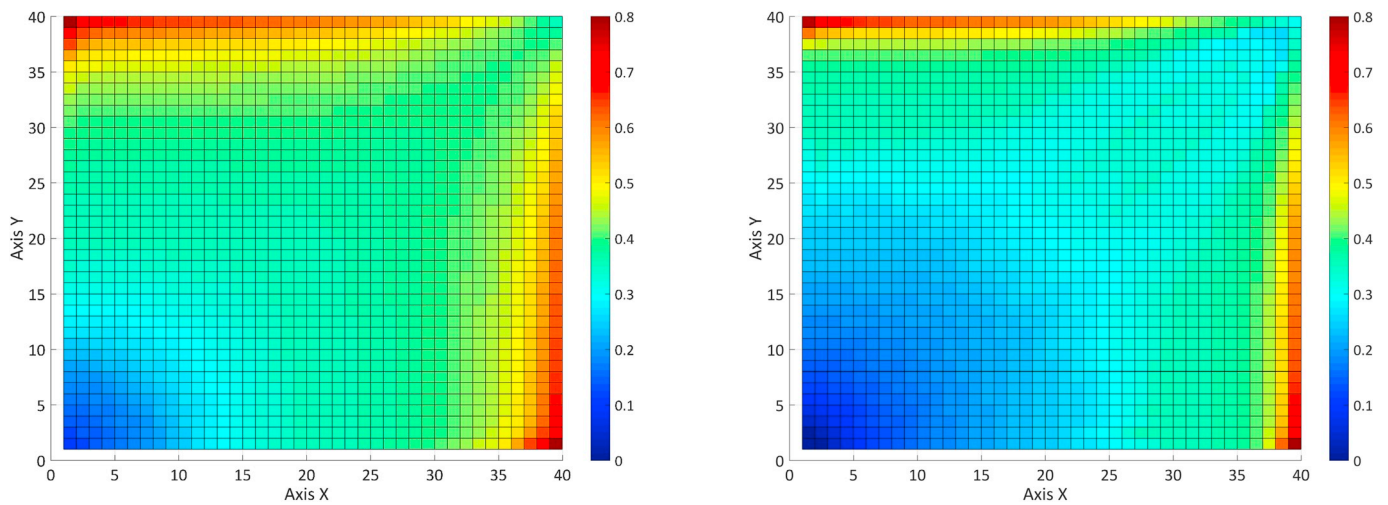


Fig. 8. Oil saturation after 3,000 days for the nanoparticles and polymer flooding (0–100/500-600 days - left) and nanoparticles and polymer flooding (0–400/50-150 days - right) schemes.

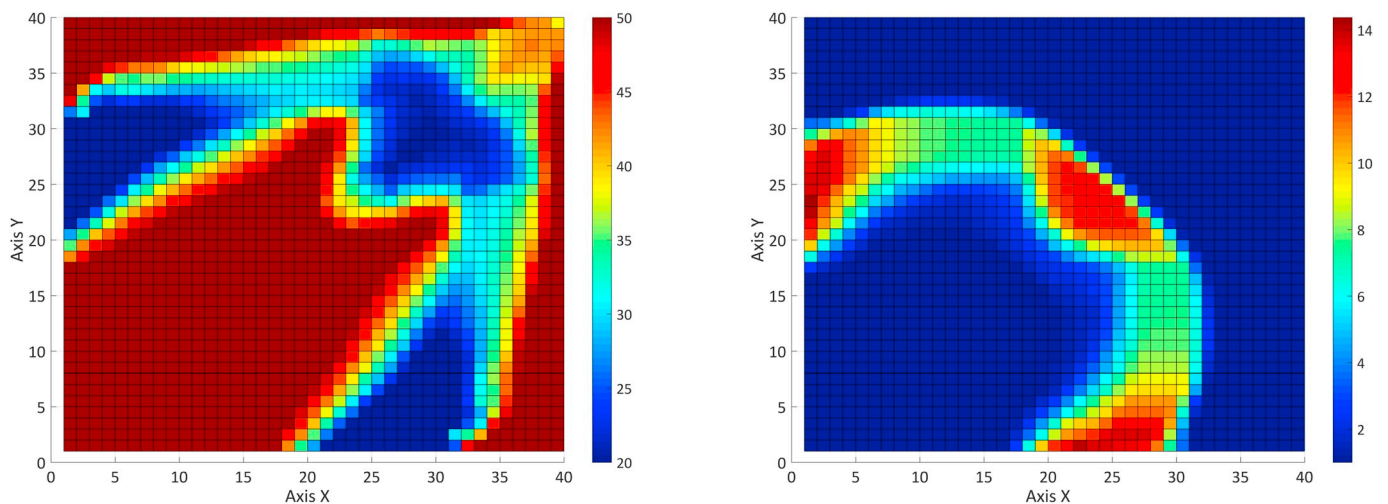


Fig. 9. Interfacial tension [mN/m] after 1,000 days for the nanoparticles and polymer flooding (0–400/300-400 days - left) and aqueous phase viscosity after 500 days for the polymer and nanoparticles flooding (0–100/50-150 days - right) schemes.

promising results. This concept of combining nanotechnology with different EOR methods has already been reported and results indicate that a whole new range of techniques can be developed using the advantages of nanoparticles (Onyekonwu and Ogolo, 2010).

The goal in this paper is to study this new EOR method, so it is vital

to understand how both products interact with the porous medium as well as with each other, i.e., their synergy. In the case of nanoparticles with the polymer something similar to the surfactant-polymer interaction (SPI) takes place. The most important property affected by both is viscosity: both nanoparticles and polymer increase the latter. For this

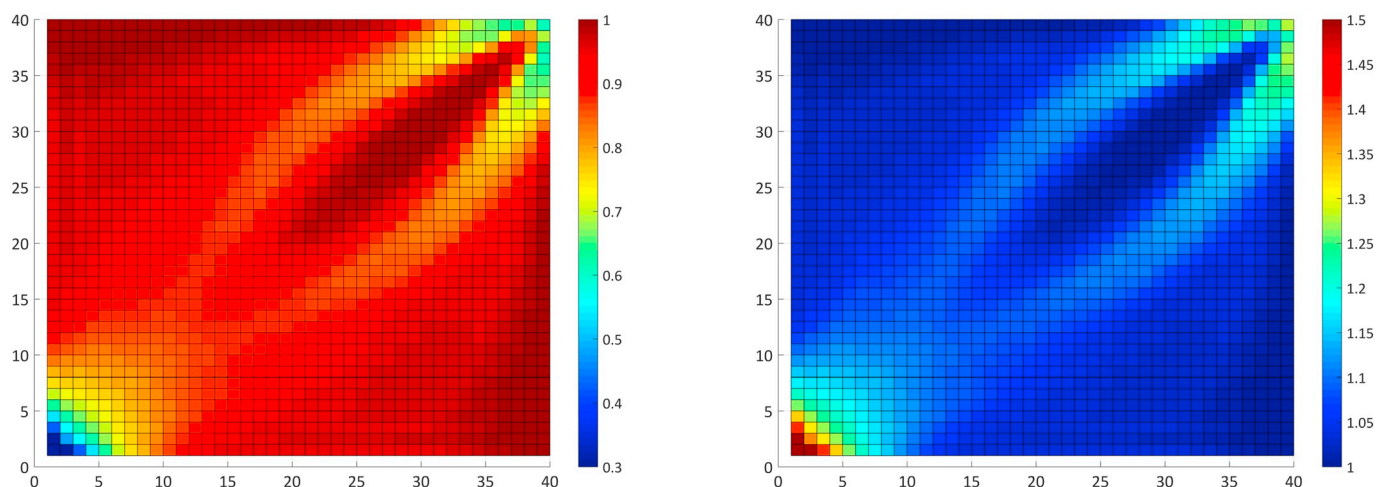


Fig. 10. Relative permeability alteration factors of the aqueous (left) and oil (right) phases after 3,000 days for the nanoparticles and polymer flooding (0–400/50–150 days) scheme.

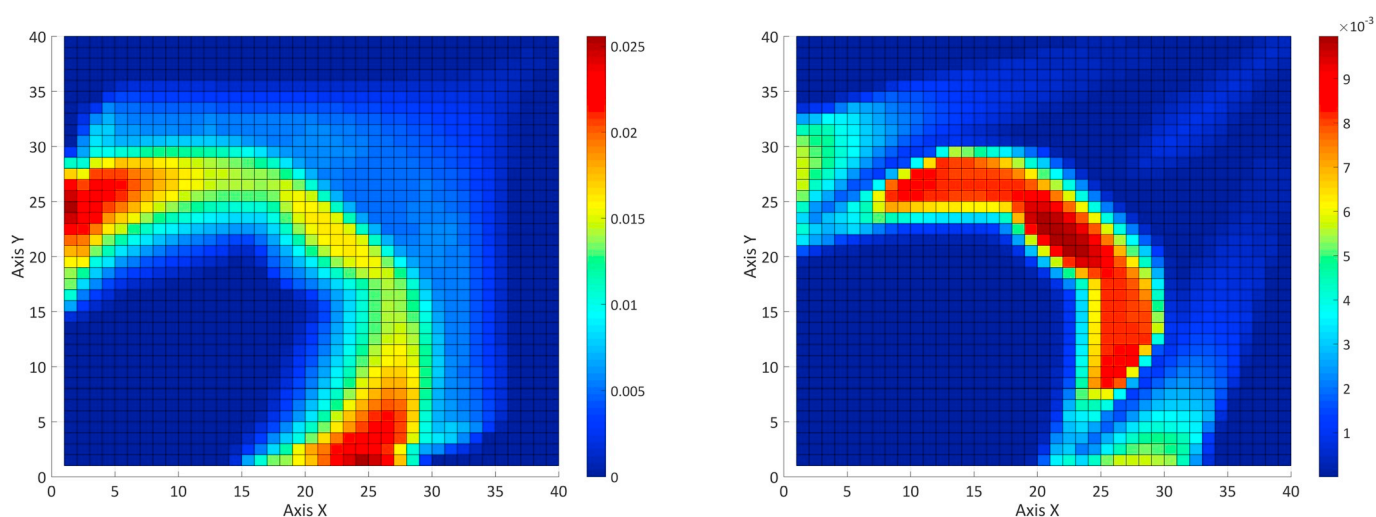


Fig. 11. Combined chemical concentrations after 750 days for the nanoparticles and polymer flooding (0–400/300–400 days - left) and after 1,000 days for the polymer and nanoparticles flooding (0–100/500–600 days - right) schemes.

simulator a sequential strategy was chosen to calculate the contribution of both chemical species to the viscosity of the water-phase. Nonetheless, in the particular case of associative polymers, the influence of these together with nanoparticles may cause an initial increase of the viscosity and then, when passing a critical nanoparticle concentration, register a decrease (Choi et al., 2017; Saito et al., 2012; Zhu et al., 2014). In the simulator the viscosity is directly proportional to both concentrations. Future developments of polymer/nanoparticles simulators should consider the special influence of associative polymer when modeling the rheology behavior.

The other two properties affected are the nanoparticles' diffusion coefficient and the adsorption onto the rock formation. The diffusion coefficient calculation starts from the basis of the Einstein-Stokes equation for spherical particles, which is currently used in nanoparticles simulators (Sbai and Azaroual, 2011; El-Amin et al., 2015; Ju and Fan, 2009). However, there is a correction for this formula considering the concentration of the particles (Eq. (12)). Together with this factor it was also considered the influence of the polymer on the solution concerning the diffusion coefficient of the particles. According to the geometry of the polymer molecules the latter is affected (Omari et al., 2009; Dong et al., 2015; Kohli and Mukhopadhyay, 2012; xian Li et al., 2016). In order to take this into account it is necessary to calculate the radius of gyration of the polymer molecules, according to the

formulation presented in this paper (Eqs. (13)–(17)). In the case of adsorption the species injected first are adsorbed onto the porous medium, limiting the surface of available rock for future adsorption processes of the subsequent EOR agents. This was considered including a factor that takes into account this competitive adsorption process in the Langmuir isotherms.

The simulation technique comprise several scenarios. First, a constant permeability field was used to compare different injection schemes of nanoparticles and polymers, which can be divided into: polymer and nanoparticles (separated/overlapped) and vice versa. In this case, it is evident that the first-injection of the nanoparticles has a beneficial effect in several senses, namely: it decreases the amount of polymer adsorbed by the rock, maintaining the mobility factor in reasonable values as well as modifying the wettability of the rock, increasing hereby the recovery efficiency. The initial slight decrease in the viscosity of the nanofluid is compensated later with the polymer injection. The operating conditions and physical properties of the phases involved are maintained from the previous section. Table 4 and Fig. 6 present the results of the simulations under different injection schemes.

When the time difference between chemical injection periods increases, the process tends to become as two EOR chemical flooding processes, without considering their synergy, except in the adsorption

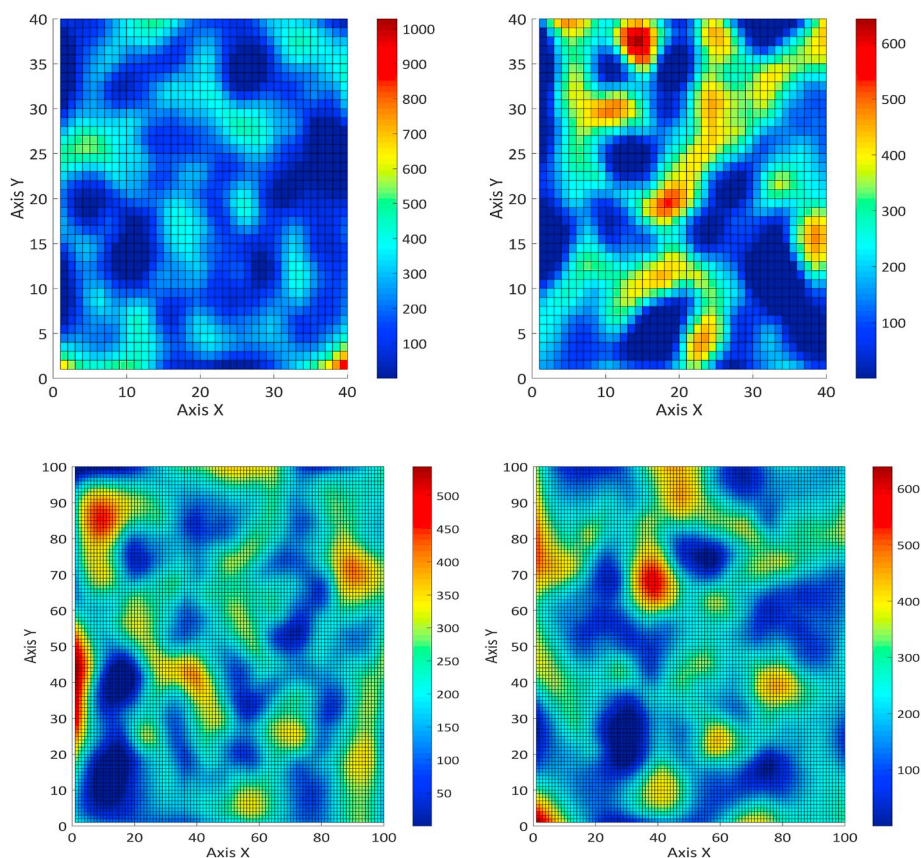


Fig. 12. Absolute permeability fields in the X (left) and Y (right) directions for two oil fields, using a different spatial grid, expressed in mD.

Table 5

Results of the recovery process for different combined polymer and nanoparticles flooding in a random permeability medium.

Case (injection scheme)	Oil recovered		Remarks
days	m ³	%OOIP	–
Pol. + NP (0–100/500–600)	53,060	28.3	–
Pol. + NP (0–100/50–150)	56,110	29.9	–
NP + Pol. (0–100/500–600)	49,330	26.3	–
NP + Pol. (0–400/50–150)	68,220	36.4	–
NP + Pol. (0–400/50–150)	65,390	34.9	Salt as 5th component

mechanisms. While all results evidence an improvement over the reference case, the best results were obtained when the chemicals were injected with an overlap, or even simultaneously (Figs. 7 and 8). Following the optimization process, several injection schemes were simulated in order to find an optimal result, in terms of injected chemical and oil recovered. Taking this into account, the best result was obtained when the nanoparticles were first injected, as discussed in the previous paragraph, but using a different injection and concentration strategies than in previous cases.

Nanoparticles do not act primarily as a viscosifying agent but as a means to alter wettability and reduce the interfacial tension (Figs. 9 and 10). If a slug of nanoparticles is injected for a longer time with a lower concentration, the wettability change is achieved before the polymer is injected (Fig. 10). When the latter begins to sweep the residual oil, it is in a medium with a lower interfacial energy and wettability suitable for the oil phase displacement. This, coupled with the viscosity of the polymer/nanofluid solution, achieves very low mobility ratios in the injection zone which then extend to the entire oil field (Figs. 10 and 11).

Two different combined chemical concentration patterns are

presented in Fig. 11. Comparing the residual oil saturations between the overlapped injection models, it becomes evident that, when the polymer was injected first, the loss of viscosity due to adsorption was greater. This, along with the interfacial properties, caused higher residual saturations than in the inverse case. In addition, when the polymer was injected in the first order, the injection scheme of the nanoparticles was modified back to the original one. Due to the fact that nanoparticles are now in the last slug, the interfacial properties together with the rheology should be the best possible in order to achieve the best oil displacement after the polymer slug. Nevertheless, the viscosifying capabilities of the nanoparticles cannot achieve residual oil saturations values similar to those with the polymer, decreasing the recovery efficiency. The influence of the competitive adsorption also plays an important role in this new combined process, so its behavior in laboratory tests should also be the object of future research.

The last part of the simulations consists of repeating the injection schemes in a porous medium with a random permeability field in order to verify the results and trends. Two porous media were designed with different random permeability fields: the first one using the same spatial grid as before, and the second is a field of the same physical dimensions but with a refined mesh aimed at testing as well the computational capacity of the simulator (Fig. 12).

The injection schemes are those from previous cases, adding an extra case for overlapped injection considering the presence of the salt as a fifth component, which allowed studying its influence on the recovery process, especially with respect to the adsorption. Results for the non-refined mesh are shown in Table 5 and Figs. 13–15. The behavior observed was similar to those obtained previously. The addition of salt in the model caused a slight reduction of the oil recovered due to greater adsorption rates of the chemical species, which depend on the TDS.

The oil saturation profiles presented in Fig. 14 depict how different

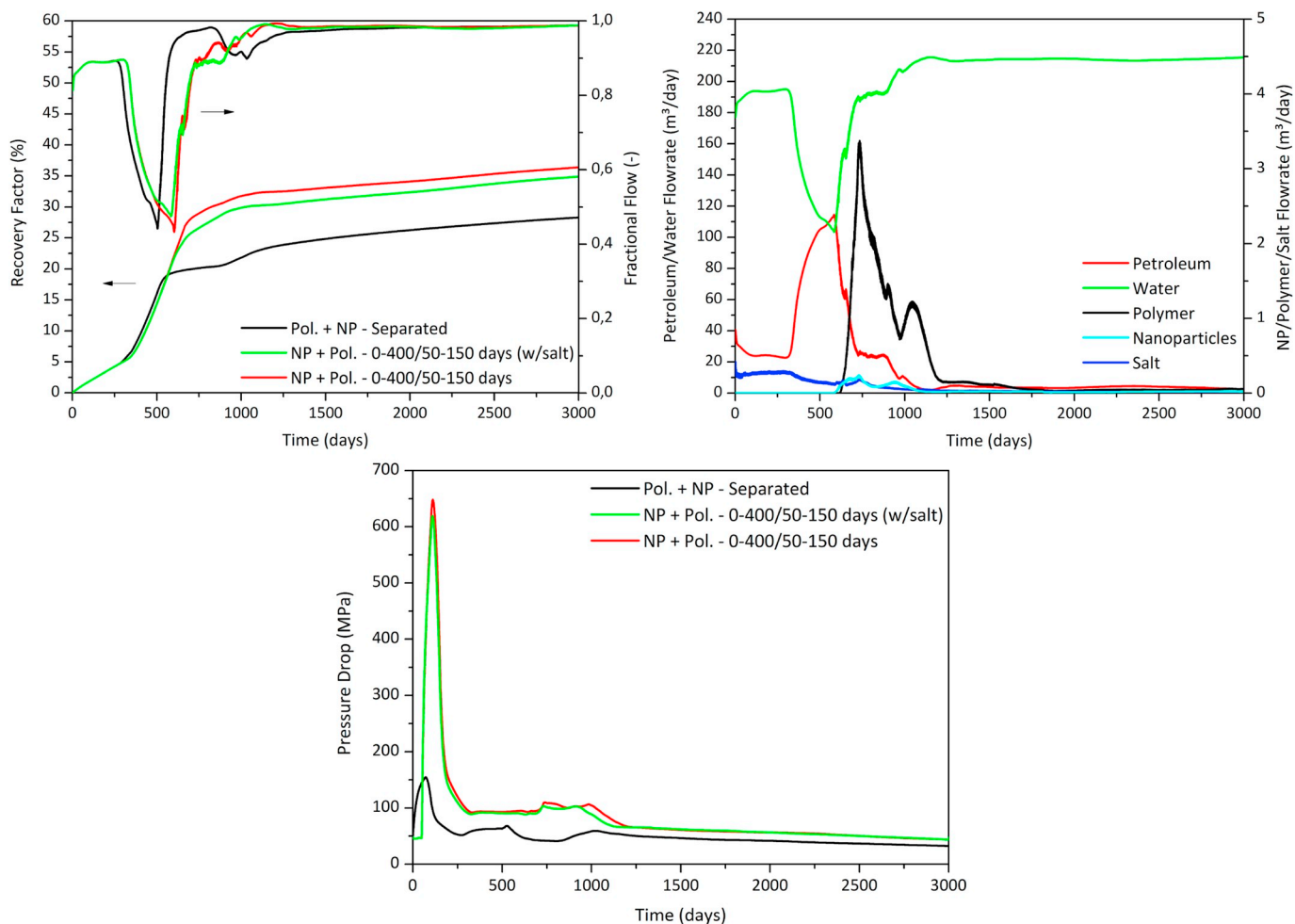


Fig. 13. Oil recovery, fractional flow (top left), flowrates for the five-component case (top right), and pressure drop (bottom) as a function of time for different combined cases in a random medium.

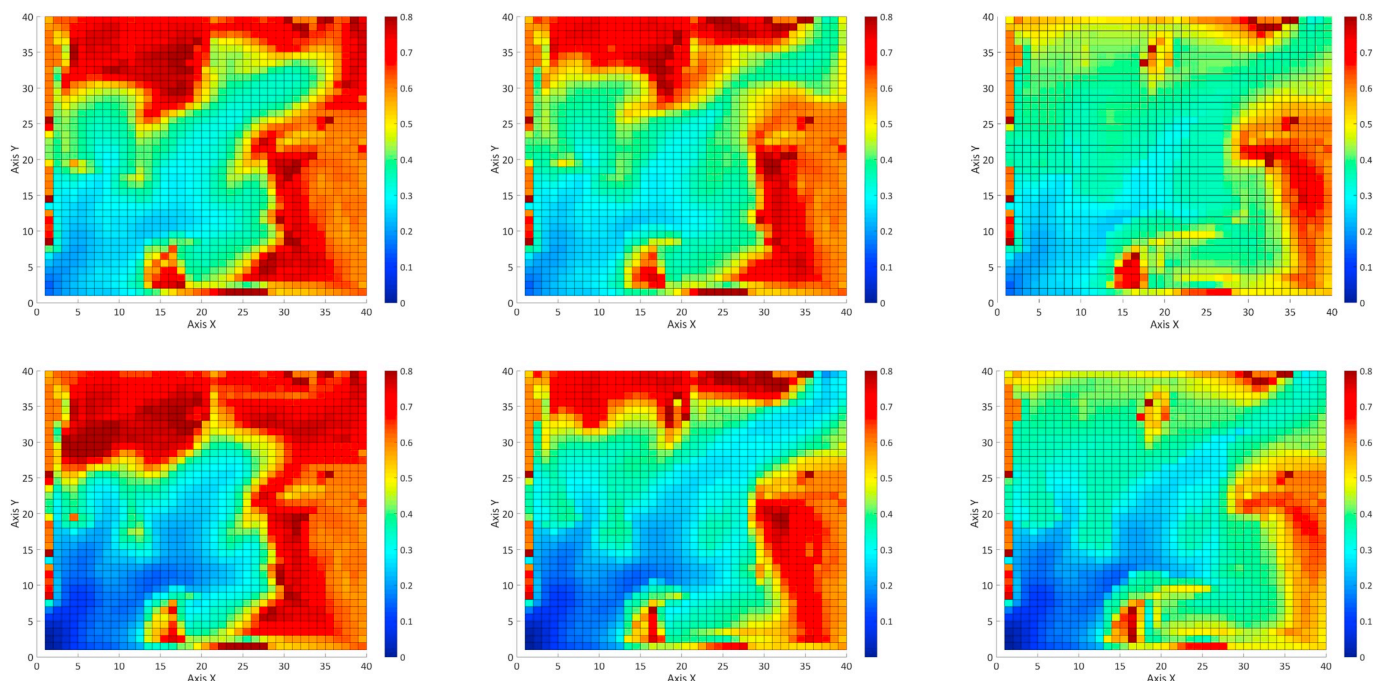


Fig. 14. Oil saturation profiles after 500 (left), 1,000 (middle) and 3,000 (right) days for a polymer and nanoparticles (0–100/500–600 days) process (top) and the nanoparticles and polymer case with salt as the 5th component (bottom).

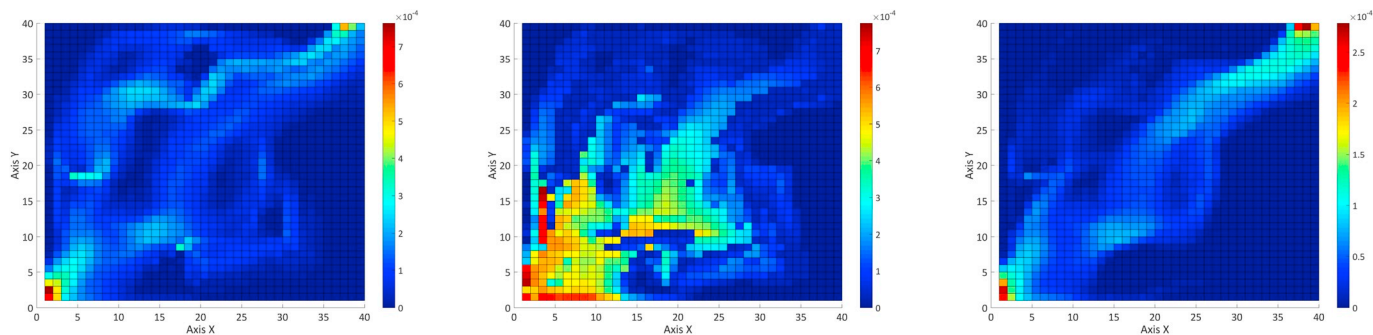


Fig. 15. Nanoparticles adsorbed for the polymer and nanoparticles overlapped process (0–100/50-150 days - left), and adsorbed polymer (middle) and nanoparticles (right) for the separated injection scheme (0–100/500-600 days).

Table 6

Results of the recovery process for different combined flooding schemes and the reference cases in the refined mesh.

Case	Oil recovered		Case	Oil recovered	
days	m ³	%OOIP	days	m ³	%OOIP
Reference Waterflooding	46,350	24.7	Pol. + NP (0–100/50-150)	79,700	42.5
Reference Polymer	63,370	33.8	NP + Pol. (0–400/50-150)	84,050	44.8

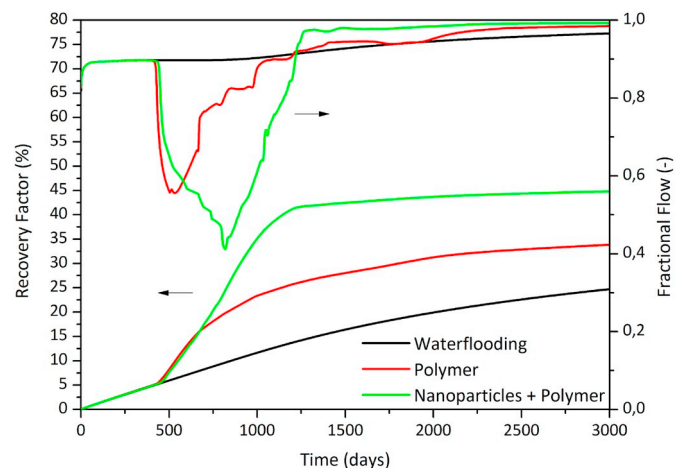


Fig. 16. Oil recovery and fractional flow as a function of time for the reference cases and the nanoparticles and polymer scheme in the refined mesh.

injection schemes can affect the recovery efficiency. In the case with salt present (Fig. 14 - bottom), even though the latter increased the adsorption rates, decreasing the oil recovered, the final recovery factor is significantly higher than when chemicals were injected separately (Fig. 14 - top). The adsorption rates of two dissimilar models with different injection orders were also studied (Fig. 15). When both chemical were injected at the same time (Fig. 15 - left), the nanoparticles adsorption was noticeable higher. On the other hand, when the polymer was injected first acted as sacrificing agent, reducing considerably de adsorption rate (Fig. 15 - middle and right).

Finally, the refined mesh is used to simulate the most relevant schemes presented so far. The objective of these simulations is to test the simulator with large and sparse matrices in order to assess its efficiency in solving these systems. The injection schemes tested are the reference cases (i.e., waterflooding and linear polymer) and two overlapped chemical EOR flooding processes enhanced by means of the nanotechnology. The results are presented in Table 6 and Figs. 16–22.

Figs. 17 and 18 present the oil saturation profile at different stages

of two EOR processes and at the end of the simulation for the cases depicted in Fig. 16, respectively. The waterflooding used as reference did not achieve in the area nearby the injection well a residual oil saturation similar to those achieved by the EOR techniques. Moreover, the fingering is still noticeable at the end of the simulation (Fig. 18 - left) whilst in the other two cases, reference polymer and NPs and polymer, the lower mobility ratio decreased the presence of fingers (Fig. 18 - middle and right).

The presence of both chemicals altered the properties of the porous medium, as depicted in Figs. 19 and 20. The polymer affected the permeability of the water-phase due to the already discussed DPR, which is related as well to its adsorption onto the rock formation (Fig. 19). On the other hand, the nanoparticles alter the wettability of the medium due to the adsorption, modifying as well the porosity and the absolute permeability (Fig. 20). These processes affect the pressure field, increasing the pressure drop between injector and producer when compared to waterflooding (Fig. 21).

The interfacial energy is affected by the nanoparticle slug as it displaces the oil from the injector to the producer (Fig. 22), which increases the capillary and thus decreases the residual oil saturation. This is swept by the polymer slug coming after the nanoparticles. As conclusion of these simulations, the synergy between polymers and nanoparticles presents great potential to develop a new technique in chemical EOR. The possibility of using the advantages of both products rendered an increase in the recovery factor up to 20.11% and 11.03% of the OOIP with respect to the reference cases, water- and linear polymer flooding, respectively. Thus, it is recommended that the injection of the chemical species be done simultaneously or overlapped, with the nanoparticles first in order to achieve a modification of the wettability (in the case of oil-wet rocks) so that the polymer can later sweep the remaining oil taking advantage of its viscosifying and viscoelastic properties as well as the improved interfacial ones caused by the presence of nanoparticles.

The last part of this paper consists in a sensitivity analysis of the main parameters involved in the proposed combined EOR process with nanoparticles. It is evident from Tables 1–3 that a complete sensitivity analysis of all the factors involved in a chemical EOR recovery would involve a significant number of simulations, carrying out either a one-factor-at-a-time (OFAT) analysis or by means of several dimensionless groups. Since the goal in this study is to present this new technique and analyze the advantages of the combined use of polymers with nanoparticles, the scope of the sensitivity analysis will be limited to the injection parameters, i.e., the injection times and the EOR agents' concentrations. Thus, the first analysis, presented in Table 7, deals with the influence of the difference between the EOR agents' injection times.

The difference in the injection time has a notorious influence in the recovery efficiency. As this time gap is increased, the whole process tends to behave as two EOR methods acting separately in the oilfield, and thus the combined efficiency of the products is not exploited. As mentioned in the literature for different recovery techniques, the

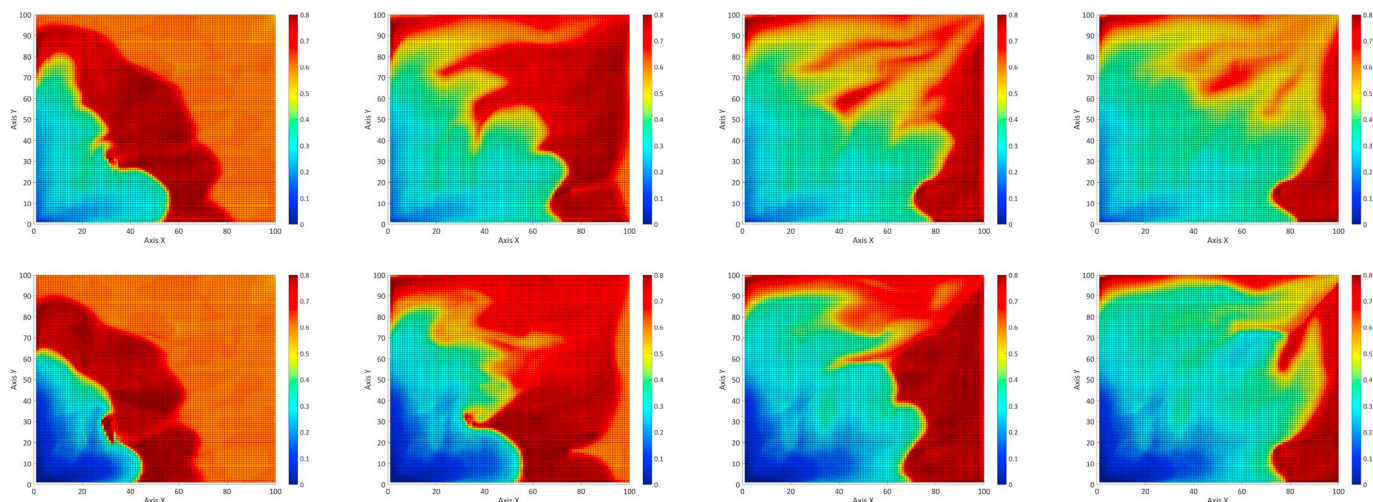


Fig. 17. Oil saturation after 250 (left), 500 (middle left), 750 (middle right) and 1,000 days (right) of simulation for the linear polymer (top) and the nanoparticle and polymer (bottom) EOR flooding processes.

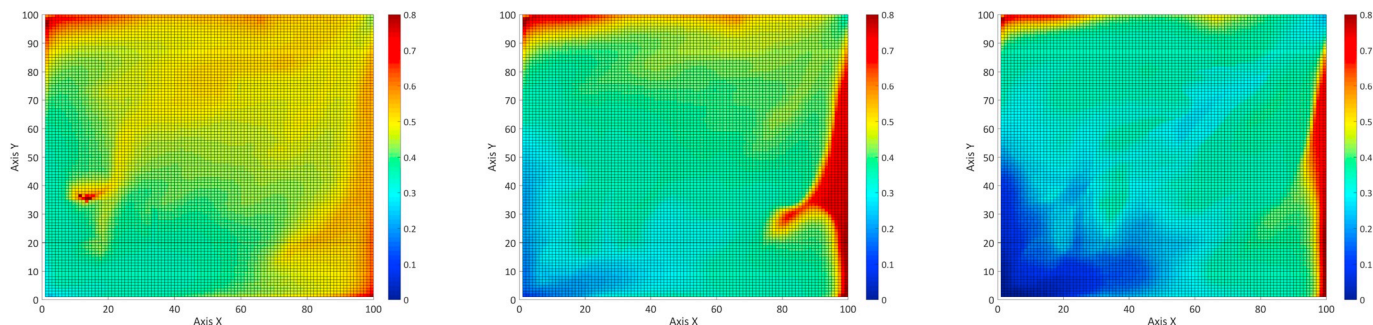


Fig. 18. Oil saturation after 3,000 days for the waterflooding (left), linear polymer (middle) and the nanoparticle and polymer (right) EOR flooding schemes.

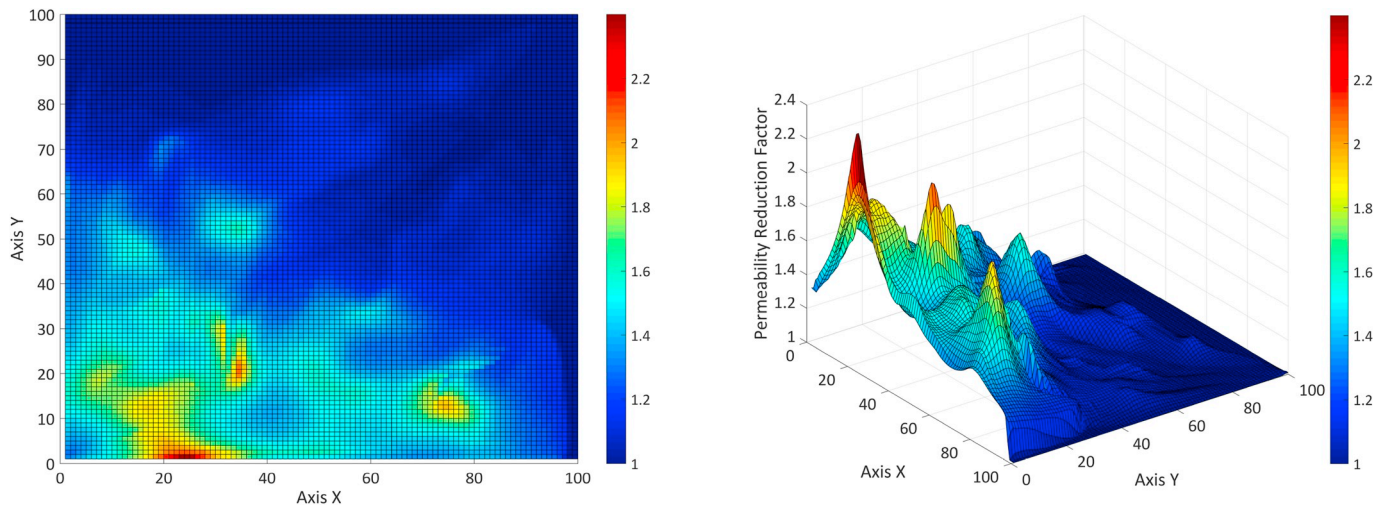


Fig. 19. DPR factor after 3,000 days for the nanoparticles and polymer flooding case.

difference between the injection times must be as short as possible in order to take advantage of the synergy between the EOR products. This is more evident in the cases when the nanoparticles are injected first, since their adsorption onto the rock matrix produces the wettability modification, altering the relative permeabilities and thus increasing the effectiveness of the subsequent polymer flooding. With respect to random permeability field, it is noted in Table 5 that the time difference in the injection also affects the recovery efficiency, although to a lesser extent. This is due to the fact that the permeability field hinders the

performance of EOR agents, which is a well-known phenomenon in oil recovery processes, in both separated and overlapped flooding schemes.

The second part of this analysis presents the influence of the injection time/concentration of the nanoparticles. The different cases presented in this paper considered the same total amount of nanoparticles injected into the system, varying the period and thus its concentration (Table 8).

The nanoparticles' injection period also shows an influence on the recovery efficiency, of the same order as the one presented in Table 7.

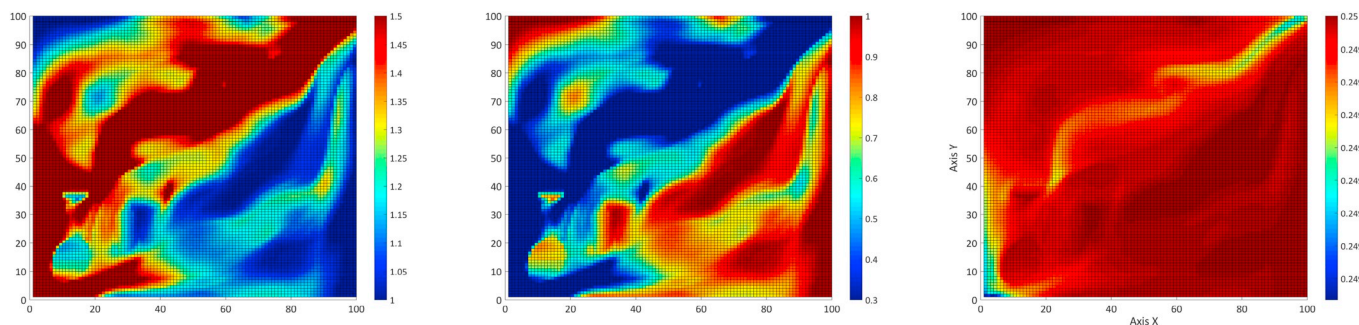


Fig. 20. Factors affecting the relative permeabilities of the oil (left), aqueous (middle) phases and porosity (right) in the nanoparticles and polymer flooding case.

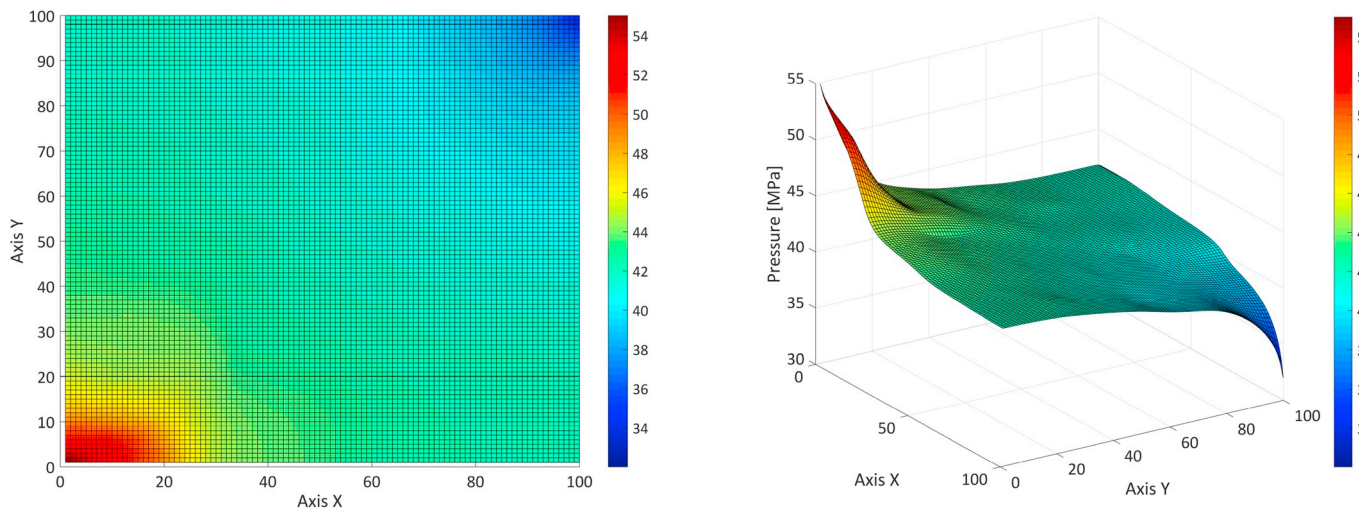


Fig. 21. Pressure field after 3,000 days for the linear polymer flooding scheme.

Even though higher concentrations increase the water viscosity, the influence of the nanoparticles on the rheological properties is not significant and therefore, the recovery efficiency is not largely affected. As mentioned before, the major role of the nanoparticles in EOR processes is the rock wettability modification, increasing the oil mobility. The extension of the wettability alteration in the oilfield depends on the injection parameters, affecting the efficiency of the process. Moreover, by increasing the injection time, the gap between EOR agents is reduced and the process exploits to a greater extent the synergy between polymer and nanoparticles.

4. Conclusions

This paper aimed at introducing a new combined recovery process in EOR, using the nanotechnology to boost a traditional chemical flooding with polymers. Thus, a mathematical model was developed for a 2D domain, with two-phases and five-components. This model considers as well the interaction between the chemical species present in the reservoir, which has a notorious effect in the nanoparticles diffusion coefficient and in the adsorption. In this last case, this interaction was modeled similarly as the well-known surfactant-polymer interactions (SPI). The physical model was described by a system of non-linear differential equations, which are solved by the finite difference method, elaborating an algorithm which was implemented in MATLAB™. The discretization of the differential equations was made using a second-order stencil with flux limiters, which decrease the influence of numerical diffusion and dispersion, achieving a better front-tracking of the chemical slugs. The simulations were aimed at understanding how the polymers’ architecture affect the recovery factor, the advantages of using nanoparticles in EOR processes, and finally study the synergy of using a novel combined method with polymers and nanoparticles. This

included an analysis of the efficiency under different injection schemes and the reasons of the mechanisms leading to the highest recovery factor.

The combined simulation of nanoparticles and polymer permitted identifying the synergies and advantages of using both products together, which, to our best knowledge, had not been previously reported. The ability of the particles to alter the wettability of the rock as well as to reduce the interfacial energy allows the polymer slug to sweep the oil bank more easily. The phenomenon of competitive adsorption works in this case as an advantage for the proposed method, provided the nanoparticles are injected in the first place: the latter change the porous medium wettability to water-wet or strongly water-wet, while the viscosifying properties are not significantly affected because the polymer is the main actor in this aspect. Nonetheless, there are certain points requiring further analysis, namely: the viscosity model in case of the presence of nanoparticles with associative polymers, an improved adsorption model in case of HLPN particles, a new model for the interfacial tension in the presence of nanoparticles and polymers, and further research in the case of nanoparticles with polymeric surfactants.

All things considered, nanotechnology-enhanced polymer flooding could represent a novel and improved technique in chemical EOR process, considering the advantages and the synergy of both products working together. The next step is to proceed with laboratory trials in order to verify the feasibility of the proposed method. This can be coupled with the recently developed “green” polymers, hydrophobically modified polymers and polymeric surfactants. Nanotechnology represents a breakthrough in EOR processes and it is a perfect example of how already well-developed techniques can be enhanced by using the advantages at the nanoscale.

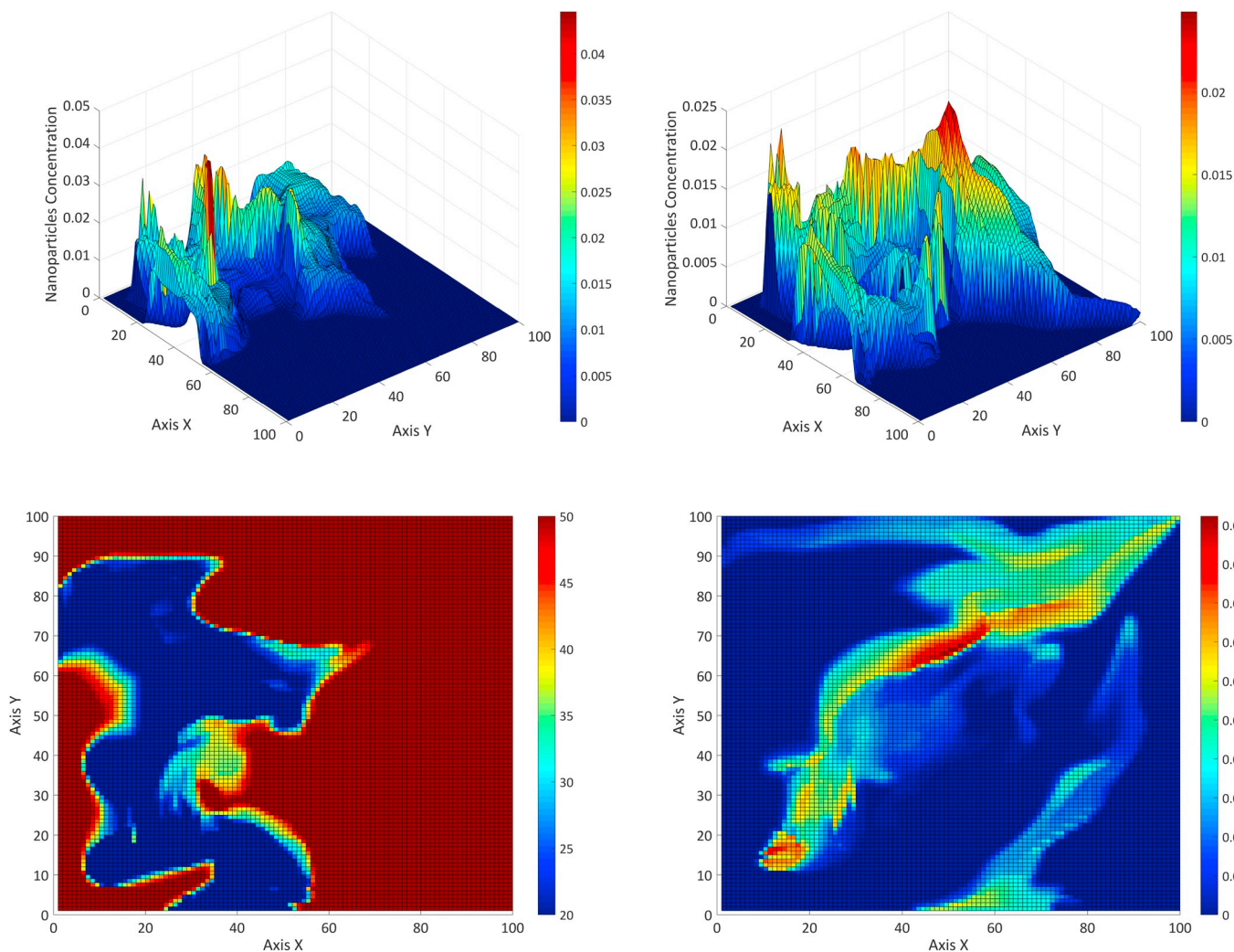


Fig. 22. Nanoparticles concentration after 500 (top left), 750 (top right) and 1,000 days (bottom right), and IFT after 500 days [mN/m] (bottom left) for the nanoparticles and polymer flooding scheme.

Table 7
Sensitivity analysis for the difference between injection times.

Case (Δt_{inj})	Oil recovered	Difference	Case (Δt_{inj})	Oil recovered	Difference
days	%OOIP	%	days	%OOIP	%
Pol. + NP (500)	35.4	–	NP + Pol. (500)	32.3	–
Pol. + NP (250)	36.1	0.7	NP + Pol. (300)	40.7	8.4
Pol. + NP (100)	37.9	2.5	NP + Pol. (150)	43.5	11.2
Pol. + NP (50)	38.3	2.9	NP + Pol. (50)	44.4	12.1

Table 8
Sensitivity analysis for the difference between injection times and concentrations.

NP Inj. Time	NP Inj. Concentration	Oil recovered	Difference
days	–	%OOIP	%
100	0.2	37.3	–
200	0.1	39.2	1.9
400	0.05	40.7	3.4

Acknowledgments

P.D. gratefully acknowledges the support of the Erasmus Mundus EURICA scholarship program (Program Number 2013-2587/001-001-

EMA2) and the Roberto Rocca Education Program. The authors would like to thank the editors and reviewers for their insightful comments on the paper, as these led us to an improvement of our work.

References

Anne-Archard, D., d’Olce, M., Tourbin, M., Frances, C., 2013. Aggregation of silica nanoparticles in concentrated suspensions under turbulent, shear and extensional flows. *Chem. Eng. Sci.* 95, 184–193. <https://doi.org/10.1016/j.ces.2013.03.005>.
 Barrett, R., Berry, M., Chan, T., Demmel, J., Donato, J., Dongarra, J., Eijkhout, V., Pozo, R., Romine, C., der Vorst van, 1994. *Templates for the Solution of Linear Systems: Building Blocks for Iterative Methods*. Society for Industrial and Applied Mathematics 978-0-89871-328-2 <https://doi.org/10.1137/1.9781611971538>.
 Berret, J., Yokota, K., Morvan, M., 2004. Interactions between polymers and nanoparticles: formation of “supermicellar” hybrid aggregates. *Soft Mater.* 2 (2–3), 71–84. <https://doi.org/10.1081/SMTS-200056090>.

- Berry, G., 1967. Thermodynamic and conformational properties of polystyrene .2. Intrinsic viscosity studies on dilute solutions of linear polystyrenes. *J. Chem. Phys.* 46 (4). <https://doi.org/10.1063/1.1840854>. 1338–&.
- Berry, G., 1968. Translational frictional constant of comb-branched polymers. *J. Polym. Sci. 2 Polym. Phys.* 6 (8PA2). <https://doi.org/10.1002/pol.1968.160060811>. 1551–&.
- Berry, G., 1971. Thermodynamic and conformational properties of polystyrene .3. Dilute solution studies on branched polymers. *J. Polym. Sci. 2 Polym. Phys.* 9 (4). <https://doi.org/10.1002/pol.1971.160090410>. 687–&.
- Bidner, M.S., Savioli, G.B., 2002. On the numerical modeling for surfactant flooding of oil reservoirs. *Mecanica Computacional XXI*, 566–585.
- Brunelli, A., Pojana, G., Callegaro, S., Marcomini, A., 2013. Agglomeration and sedimentation of titanium dioxide nanoparticles (n-TiO₂) in synthetic and real waters. *J. Nanoparticle Res.* 15 (6), 1684. <https://doi.org/10.1007/s11051-013-1684-4>.
- Capco, D.G., Chen, Y., 2014. *Nanomaterial*. Springer, Dordrecht, the Netherlands.
- Chen, Z., Huan, G., Ma, Y., 2006. *Computational Methods for Multiphase Flows in Porous Media*. Society for Industrial and Applied Mathematics 978-0-89871-606-1 <https://doi.org/10.1137/1.9780898718942>.
- Choi, S.K., Son, H.A., Kim, H.T., Kim, J.W., 2017. Nanofluid enhanced oil recovery using hydrophobically associative zwitterionic polymer-coated silica nanoparticles. *Energy Fuels* 31 (8), 7777–7782. <https://doi.org/10.1021/acs.energyfuels.7b00455>.
- Dake, L.P., 1978. *Fundamentals of Reservoir Engineering*. Elsevier, Amsterdam, the Netherlands 0-444-41830-X.
- Delshad, M., Pope, G., Sepehrnoori, K., 2000. *UTCHEM Version 9.0 Technical Documentation*. Center for Petroleum and Geosystems Engineering, The University of Texas at Austin, USA 78751.
- Dong, Y., Feng, X., Zhao, N., Hou, Z., 2015. Diffusion of nanoparticles in semidilute polymer solutions: a mode-coupling theory study. *J. Chem. Phys.* 143 (2), 024903. <https://doi.org/10.1063/1.4926412>.
- Druetta, P., Picchioni, F., 2018. Numerical modeling and validation of a novel 2D compositional flooding simulator using a second-order TVD scheme. *Energies* 11, 2280. <https://doi.org/10.3390/en11092280>.
- Druetta, P., Picchioni, F., 2019. Influence of the polymer degradation on enhanced oil recovery processes. *Appl. Math. Model.* 69, 142–163. <https://doi.org/10.1016/j.apm.2018.11.051>.
- Druetta, P., Yue, J., Tesi, P., Persis, C.D., Picchioni, F., 2017. Numerical modeling of a compositional flow for chemical EOR and its stability analysis. *Appl. Math. Model.* 47, 141–159. <https://doi.org/10.1016/j.apm.2017.03.017>.
- Druetta, P., Raffa, P., Picchioni, F., 2018. Plenty of room at the bottom: nanotechnology as solution to an old issue in enhanced oil recovery. *Appl. Sci.* 8, 2596. <https://doi.org/10.3390/app8122596>.
- Duan, F., Kwek, D., Crivoi, A., 2011. Viscosity affected by nanoparticle aggregation in Al₂O₃-water nanofluids. *Nanoscale Research Letters* 6, 248. <https://doi.org/10.1186/1556-276X-6-248>.
- El-Amin, M.F., Meftah, R., Salama, A., Sun, S., 2015. Numerical treatment of two-phase flow in porous media including specific interfacial area. *Procedia Computer Science* 51, 1249–1258.
- Graessley, W.W., 1977. Effect of long branches on the flow properties of polymers. *Accounts Chem. Res.* 10 (9), 332–339.
- Graessley, W., Masuda, T., Roovers, J., Hadjichristidis, N., 1976. Rheological properties of linear and branched polyisoprene. *Macromolecules* 9 (1), 127–141. <https://doi.org/10.1021/ma60049a025>.
- Jia-Fei, Z., Zhong-Yang, L., Ming-Jiang, N., Ke-Fe, C., 2009. Dependence of nanofluid viscosity on particle size and pH value. *Chin. Phys. Lett.* 26 (6), 066202.
- Jiang, W., Ding, G., Peng, H., Hu, H., 2010. Modeling of nanoparticles' aggregation and sedimentation in nanofluid. *Curr. Appl. Phys.* 10 (3), 934–941. <https://doi.org/10.1016/j.cap.2009.11.076>.
- Ju, B., Fan, T., 2009. Experimental study and mathematical model of nanoparticle transport in porous media. *Powder Technol.* 192 (2), 195–202. <https://doi.org/10.1016/j.powtec.2008.12.017>.
- Ju, B., Fan, T., 2013. Experimental study on nanoparticles transport and its effects on two-phase flow behavior in porous networks. *Part. Sci. Technol.* 31 (2), 114–118. <https://doi.org/10.1080/02726351.2012.669028>.
- Ju, B., Fan, T., Ma, M., 2006. Enhanced oil recovery by flooding with hydrophilic nanoparticles. *China Particuol.* 4 (01), 41–46.
- Kamalyar, K., Kharrat, R., Nikbakht, M., 2014. Numerical aspects of the convection-dispersion equation. *Petrol. Sci. Technol.* 32 (14), 1729–1762. <https://doi.org/10.1080/10916466.2010.490802>.
- Kang, H., Zhang, Y., Yang, M., Li, L., 2012. Molecular dynamics simulation on effect of nanoparticle aggregation on transport properties of a nanofluid. *J. Nanotechnol. Eng. Med.* 3 (2), 021001.
- Khandavalli, S., Rothstein, J.P., 2014. Extensional rheology of shear-thickening fumed silica nanoparticles dispersed in an aqueous polyethylene oxide solution. *J. Rheol.* 58 (2), 411–431. <https://doi.org/10.1122/1.4864620>.
- Kohli, I., 2013. *Dynamics of Gold Nanoparticles in Synthetic and Biopolymer Solutions*. Doctoral dissertation. Wayne State University, USA.
- Kohli, I., Mukhopadhyay, A., 2012. Diffusion of nanoparticles in semidilute polymer solutions: effect of different length scales. *Macromolecules* 45 (15), 6143–6149. <https://doi.org/10.1021/ma301237r>.
- Kondiparty, K., Nikolov, A., Wu, S., Wasan, D., 2011. Wetting and spreading of nanofluids on solid surfaces driven by the structural disjoining pressure: statics analysis and experiments. *Langmuir* 27 (7), 3324–3335. <https://doi.org/10.1021/la104204b>.
- Lake, L.W., 1989. *Enhanced Oil Recovery*. Prentice-Hall Inc., Englewood Cliffs, USA 0-13-281601-6.
- Li, L.S., 2016. *Effects of Nanoparticle Aggregation, Particle Size and Temperature of Nanofluids Using Molecular Dynamics Simulation*. Doctoral dissertation. University of Malaya, Malaysia.
- Litchfield, D.W., Baird, D.G., 2006. The rheology of high aspect ratio nano-particle filled liquids. *Rheology Reviews* 2006, 1.
- Maghzi, A., Mohebbi, A., Kharrat, R., Ghazanfari, M.H., 2013. An experimental investigation of silica nanoparticles effect on the rheological behavior of polyacrylamide solution to enhance heavy oil recovery. *Petrol. Sci. Technol.* 31 (5), 500–508. <https://doi.org/10.1080/10916466.2010.518191>.
- Markus, A.A., Parsons, J.R., Roex, E.W.M., de Voogt, P., Laane, R.W.P.M., 2015. Modeling aggregation and sedimentation of nanoparticles in the aquatic environment. *Sci. Total Environ.* 506, 323–329. <https://doi.org/10.1016/j.scitotenv.2014.11.056>.
- Markutsya, S., 2008. *Modeling and Simulation of Nanoparticle Aggregation in Colloidal Systems*. Doctoral dissertation. Iowa State University, USA.
- Maurya, N.K., Mandal, A., 2016. Studies on behavior of suspension of silica nanoparticle in aqueous polyacrylamide solution for application in enhanced oil recovery. *Petrol. Sci. Technol.* 34 (5), 429–436. <https://doi.org/10.1080/10916466.2016.1145693>.
- Metin, C., 2012. *Characterization of Nanoparticle Transport in Flow through Permeable Media*. Doctoral dissertation. University of Texas at Austin, USA.
- Meyer, J.P., Adio, S.A., Sharifpur, M., Nwosu, P.N., 2016. The viscosity of nanofluids: a review of the theoretical, empirical, and numerical models. *Heat Transf. Eng.* 37 (5), 387–421. <https://doi.org/10.1080/01457632.2015.1057447>.
- Mikkola, V., 2012. *Impact of Concentration, Particle Size and Thermal Conductivity on Effective Convective Heat Transfer of Nanofluids*. MS Thesis. Aalto University, Finland.
- Mishra, P., Mukherjee, S., Nayak, S., Panda, A., 2014. A brief review on viscosity of nanofluids. *Int. Nano Lett.* 4 (4), 109–120. <https://doi.org/10.1007/s40089-014-0126-3>.
- Morrow, N.R., 1987. A review of the effects of initial saturation, pore structure and wettability on oil recovery by waterflooding. In: *Proceedings of the North Sea Oil and Gas Reservoirs Seminar*. Graham and Trotman, London, UK, pp. 179–191.
- Nikolov, A., Kondiparty, K., Wasan, D., 2010. Nanoparticle self-structuring in a nanofluid film spreading on a solid surface. *Langmuir* 26 (11), 7665–7670. <https://doi.org/10.1021/la100928t>.
- Omari, R.A., Aneese, A.M., Grabowski, C.A., Mukhopadhyay, A., 2009. Diffusion of nanoparticles in semidilute and entangled polymer solutions. *J. Phys. Chem. B* 113 (25), 8449–8452. <https://doi.org/10.1021/jp9035088>.
- Onyekonwu, M.O., Ogolo, N.A., 2010. Investigating the use of nanoparticles in enhancing oil recovery. In: *Nigeria Annual International Conference and Exhibition*. Society of Petroleum Engineers. <https://doi.org/10.2118/140744-MS>.
- R. Pal, Modeling the viscosity of concentrated nanoemulsions and nanosuspensions, *Fluid* 1 (2), doi:10.3390/fluids1020011.
- Phillies, G., 1987. Dynamics of polymers in concentrated-solutions - the universal scaling equation derived. *Macromolecules* 20 (3), 558–564. <https://doi.org/10.1021/ma00169a015>.
- Pranami, G., 2009. *Understanding Nanoparticle Aggregation*, Doctoral Dissertation. Iowa State University, USA.
- Rudiyak, V.Y., 2013. Viscosity of nanofluids. Why it is not described by the classical theories. *Adv. Nanoparticles* 2 (03), 266.
- Saito, Y., Hirose, Y., Otsubo, Y., 2012. Size effect on the rheological behavior of nanoparticle suspensions in associating polymer solutions. *Colloid Polym. Sci.* 290 (3), 251–259. <https://doi.org/10.1007/s00396-011-2547-0>.
- Satter, A., Iqbal, G.M., Buchwalter, J.L., 2008. *Practical Enhanced Reservoir Engineering*. PennWell Books, Tulsa, USA 978-1-59370-056-0.
- Sbai, M.A., Azaroul, M., 2011. Numerical modeling of formation damage by two-phase particulate transport processes during CO₂ injection in deep heterogeneous porous media. *Adv. Water Resour.* 34 (1), 62–82. <https://doi.org/10.1016/j.advwatres.2010.09.009>.
- Shakouri, A., Ahmari, H., Hojjat, M., Heris, S.Z., 2017. Effect of TiO₂ nanoparticle on rheological behavior of poly(vinyl alcohol) solution. *J. Vinyl Addit. Technol.* 23 (3), 234–240. <https://doi.org/10.1002/vnl.21502>.
- Shanbhag, S., 2012. Analytical rheology of polymer melts: state of the art. *ISRN Materials Science* 2012 (732176). <https://doi.org/10.5402/2012/732176>. 24–&.
- Sheng, J., 2011. *Modern Chemical Enhanced Oil Recovery*. Elsevier, Amsterdam, the Netherlands 0-08-096163-0; 978-0-08096-163-7.
- Taborda, E.A., Franco, C.A., Ruiz, M.A., Alvarado, V., Cortes, F.B., 2017. Experimental and theoretical study of viscosity reduction in heavy crude oils by addition of nanoparticles. *Energy Fuels* 31 (2), 1329–1338. <https://doi.org/10.1021/acs.energyfuels.6b02686>.
- Teraoka, I., 2002. *Models of Polymer Chains, Polymer Solutions*. John Wiley & Sons, Inc., 978-0-47122-451-8 pp. 1–67. <https://doi.org/10.1002/0471224510.ch1>. 2002.
- Wasan, D., Nikolov, A., 2003. Spreading of nanofluids on solids. *Nature* 423 (6936), 156–159. <https://doi.org/10.1038/nature01591>.
- Wasan, D., Nikolov, A., Kondiparty, K., 2011. The wetting and spreading of nanofluids on solids: role of the structural disjoining pressure. *Curr. Opin. Colloid Interface Sci.* 16 (4), 344–349. <https://doi.org/10.1016/j.cocis.2011.02.001>.
- Wever, D.A.Z., Polgar, L.M., Stuart, M.C.A., Picchioni, F., Broekhuis, A.A., 2013. Polymer molecular architecture as a tool for controlling the rheological properties of aqueous polyacrylamide solutions for enhanced oil recovery. *Ind. Eng. Chem. Res.* 52 (47), 16993–17005. <https://doi.org/10.1021/ie403045y>.
- xian Li, S., jun Jiang, H., huai Hou, Z., 2016. Diffusion of nanoparticles in semidilute polymer solutions: a multiparticle collision dynamics study. *Chin. J. Chem. Phys.* 29 (5), 549–556. <https://doi.org/10.1063/1674-0068/29/cjcp1603058>.
- Zhang, T., Murphy, M.J., Yu, H., Bagaria, H.G., Yoon, K.Y., Neilson, B.M., Bielawski, C.W., Johnston, K.P., Huh, C., Bryant, S.L., 2015. Investigation of nanoparticle adsorption during transport in porous media. *SPE J.* 20 (4), 667–677. <https://doi.org/10.2118/166346-PA>.
- Zhu, D., Wei, L., Wang, B., Feng, Y., 2014. Aqueous hybrids of silica nanoparticles and hydrophobically associating hydrolyzed polyacrylamide used for EOR in high-temperature and high-salinity reservoirs. *Energies* 7 (6), 3858–3871. <https://doi.org/10.3390/en7063858>.